EUROPEAN ORGANIZATION FOR NUCLEAR RESEARCH (CERN)

CMS-HIN-15-006

Multiplicity and rapidity dependence of strange hadron production in pp, pPb, and PbPb collisions at the LHC

The CMS Collaboration[*]

Abstract

Measurements of strange hadron (K^0_S, $\Lambda + \overline{\Lambda}$, and $\Xi^- + \overline{\Xi}^+$) transverse momentum spectra in pp, pPb, and PbPb collisions are presented over a wide range of rapidity and event charged-particle multiplicity. The data were collected with the CMS detector at the CERN LHC in pp collisions at $\sqrt{s} = 7\,\text{TeV}$, pPb collisions at $\sqrt{s_{NN}} = 5.02\,\text{TeV}$, and PbPb collisions at $\sqrt{s_{NN}} = 2.76\,\text{TeV}$. The average transverse kinetic energy is found to increase with multiplicity, at a faster rate for heavier strange particle species in all systems. At similar multiplicities, the difference in average transverse kinetic energy between different particle species is observed to be larger for pp and pPb events than for PbPb events. In pPb collisions, the average transverse kinetic energy is found to be slightly larger in the Pb-going direction than in the p-going direction for events with large multiplicity. The spectra are compared to models motivated by hydrodynamics.

[*]See Appendix A for the list of collaboration members

1 Introduction

Studies of strange-particle production in high energy collisions of protons and heavy ions provide important means to investigate the dynamics of the collision process. Earlier studies of relativistic heavy ion collisions at the BNL RHIC and CERN SPS colliders indicated an enhancement of strangeness production with respect to proton-proton (pp) collisions [1, 2], which was historically interpreted to be due to the formation of a high-density quark-gluon medium [3]. The abundance of strange particles at different center-of-mass energies is in line with calculations from thermal statistical models [4–6]. In gold-gold (AuAu) collisions at RHIC, strong azimuthal correlations of final-state hadrons were observed, suggesting that the produced medium behaves like a near-perfect fluid undergoing a pressure-driven anisotropic expansion [2]. Studies of strangeness and light flavor production and dynamics in heavy ion collisions have provided further insight into the medium's fluid-like nature and evidence for its partonic collectivity [2, 7].

In recent years, the observation of a long-range "ridge" at small azimuthal separations in two-particle correlations in pp [8] and proton-lead (pPb) [9–11] collisions with high event-by-event charged-particle multiplicity (referred to hereafter as "multiplicity") has provided an indication for collective effects in systems that are an order of magnitude smaller in size than heavy ion collisions. The nature of the observed long-range particle correlations in high multiplicity pp and pPb collisions is still under intense debate [12]. While the collective flow of a fluid-like medium provides a natural interpretation [13–16], other models attribute this behavior to the initial correlation of gluons [17–21], or the anisotropic escape of particles [22].

Studies of identified particle production and correlations in high multiplicity pp and pPb collisions provide detailed information about the underlying particle production mechanism. Identified particle (including strange-hadron) transverse momentum (p_T) spectra and azimuthal anisotropies in lead-lead (PbPb) collisions at the CERN LHC have been studied [23, 24] and described by hydrodynamic models [25, 26]. Similar measurements have been performed in pPb collisions as a function of multiplicity, where an indication of a common velocity boost to the produced particles, known as "radial flow" [27, 28], and for a mass dependence of the anisotropic flow [29, 30] have been observed. When comparing pPb and PbPb systems at similar multiplicities, a stronger radial velocity boost is seen in the smaller pPb collision system [27, 30]. This could be related to a much higher initial energy density in a high multiplicity but smaller system, resulting in a larger pressure gradient outward along the radial direction, as predicted in Ref. [31]. To perform a quantitative comparison, a common average radial-flow velocity from different collision systems can be extracted from a simultaneous fit to the spectra of various particle species, based on the blast-wave model [32]. Inspired by hydrodynamics, the blast-wave model assumes a common kinetic freeze-out temperature and radial-flow velocity for all particles during the expansion of the system. The dependence of spectral shapes for identified hadrons on the multiplicity has been observed in high energy electron and proton-antiproton collisions [33, 34], but this observation was not explored extensively in the hydrodynamic context. The blast-wave fit has been studied in pp, deuterium-gold, and AuAu collisions at RHIC [35]. In pp collisions, it has been shown through studies with simulation that color reconnection processes could describe the observed multiplicity dependence of identified particle spectra [23, 36].

It is of interest to study possible collective phenomena in very high multiplicity pp collisions, as demonstrated by the observation of long-range particle correlations in these events [8]. Since pp events represent an even smaller system than pPb events, a stronger radial-flow boost might be present compared to pPb and PbPb events at a comparable multiplicity [31]. Furthermore,

in a pPb collision, the system is not symmetric in pseudorapidity (η). If a fluid-like medium is formed, its energy density could be different on the p- and Pb-going sides, which could lead to an asymmetry in the collective radial-flow effect as a function of η. Hydrodynamical models predict that the average p_T (or, equivalently, the average transverse kinetic energy $\langle KE_T \rangle$, where $\langle KE_T \rangle \equiv \langle m_T \rangle - m$, with $m_T = \sqrt{m^2 + p_T^2}$ and m the particle mass) of produced particles is larger in the Pb-going direction than in the p-going direction, while this trend could be reversed in models based on gluon saturation [37]. Measurement of identified particle p_T spectra as a function of η could thus help to constrain theoretical models.

This Letter presents measurements of strange-particle p_T spectra in pp, pPb, and PbPb collisions as a function of the multiplicity in the events. Specifically, we examine the spectra of K^0_S, Λ, and Ξ^- particles, where the inclusion of the charge-conjugate states is implied for Λ and Ξ^- particles. The data were collected with the CMS detector at the LHC. With the implementation of a dedicated high-multiplicity trigger, the pp and pPb data samples exhibit multiplicities comparable to that observed in peripheral PbPb collisions, where "peripheral" refers to ∼50–100% centrality, with centrality defined as the fraction of the total inelastic cross section. The most central collisions have 0% centrality. This overlap in mean multiplicity allows the three systems, with drastically different collision geometries, to be compared. The large solid-angle coverage of the CMS detector permits the strange-particle p_T spectra to be studied in different rapidity ranges, and thus the study of possible asymmetries with respect to the p- and Pb-going directions in pPb collisions.

2 Detector and data samples

The central feature of the CMS apparatus is a superconducting solenoid of 6 m internal diameter, which provides an axial field of 3.8 T. Within the solenoid volume are a silicon pixel and strip tracker (with 13 and 14 layers in the central and endcap regions, respectively), a lead tungstate crystal electromagnetic calorimeter (ECAL), and a brass and scintillator hadron calorimeter (HCAL), each composed of a barrel and two endcap sections. The tracker covers the pseudorapidity range $|\eta| < 2.5$. Reconstructed tracks with $1 < p_T < 10$ GeV typically have resolutions of 1.5–3% in p_T and 25–90 (45–150) μm in the transverse (longitudinal) impact parameter [38]. The ECAL and HCAL each cover $|\eta| < 3.0$ while forward hadron calorimeters (HF) cover $3 < |\eta| < 5$. Muons with $|\eta| < 2.4$ are measured with gas-ionization detectors embedded in the steel flux-return yoke outside the solenoid. A more detailed description of the CMS detector, together with a definition of the coordinate system and the relevant kinematic variables, can be found in Ref. [39]. The Monte Carlo (MC) simulation of the particle propagation and detector response is based on the GEANT4 [40] program.

The data samples used in this analysis are as follows: pp collisions collected in 2010 at $\sqrt{s} = 7$ TeV, pPb collisions collected in 2013 at $\sqrt{s} = 5.02$ TeV, and PbPb collisions collected in 2011 at $\sqrt{s_{NN}} = 2.76$ TeV, with integrated luminosities of 6.2 pb^{-1}, 35 nb^{-1}, and 2.3 μb^{-1}, respectively.

For the pPb data, the beam energies are 4 TeV for the protons and 1.58 TeV per nucleon for the lead nuclei. The data were collected in two different run periods: one with the protons circulating in the clockwise direction in the LHC ring, and one with them circulating in the counterclockwise direction. By convention, the proton beam rapidity is taken to be positive when combining the data from the two run periods. Because of the asymmetric beam conditions, the nucleon-nucleon center-of-mass in the pPb collisions moves with speed $\beta = 0.434$ in the laboratory frame, corresponding to a rapidity of 0.465. As a consequence, the rapidity of a particle in the nucleon-nucleon center-of-mass frame (y_{cm}) is detected in the laboratory frame

(y_{lab}) with a shift, $y_{\mathrm{lab}} = y_{\mathrm{cm}} + 0.465$. The pPb particle yields reported in this Letter are presented in terms of y_{cm}, rather than y_{lab}, for better correspondence with the results from the pp and PbPb collisions.

3 Selection of events and tracks

The triggers, event reconstruction, and event selection are the same as those discussed for pp, pPb, and PbPb collisions in Refs. [8, 41]. They are briefly outlined in the following paragraphs for pp and pPb collisions, which are the main focus of this Letter. A subset of peripheral PbPb data collected in 2011 with a minimum-bias trigger is reprocessed using the same event selection and track reconstruction algorithm as for the present pPb and pp analyses, in order to more directly compare the three systems at the same multiplicity. Details of the 2011 PbPb analysis can be found in Refs. [41, 42].

Minimum-bias pPb events are triggered by requiring at least one track with $p_{\mathrm{T}} > 0.4\,\mathrm{GeV}$ to be found in the pixel tracker. Because of hardware limitations in the data acquisition rate, only a small fraction $(\sim 10^{-3})$ of triggered minimum-bias events are recorded. In order to collect a large sample of high-multiplicity pPb collisions, a dedicated high-multiplicity trigger is implemented using the CMS Level-1 (L1) and high-level trigger (HLT) systems [43]. At L1, the total transverse energy summed over the ECAL and HCAL is required to exceed either 20 or 40 GeV, depending on the multiplicity requirement as specified below. Charged particles are reconstructed at the HLT level using the pixel detectors. It is required that these tracks originate within a cylindrical region (30 cm in length along the direction of the beam axis and 0.2 cm in radius in the direction perpendicular to that axis) centered on the nominal interaction point. For each event, the number of pixel tracks ($N_{\mathrm{trk}}^{\mathrm{online}}$) with $|\eta| < 2.4$ and $p_{\mathrm{T}} > 0.4\,\mathrm{GeV}$ is determined for each reconstructed vertex. Only tracks with a distance of closest approach 0.4 cm or less to one of the vertices are included. The HLT selection requires $N_{\mathrm{trk}}^{\mathrm{online}}$ for the vertex with the largest number of tracks to exceed a specific value. Data are collected in pPb collisions with thresholds $N_{\mathrm{trk}}^{\mathrm{online}} > 100$ and 130 for events with an L1 transverse energy threshold of 20 GeV, and $N_{\mathrm{trk}}^{\mathrm{online}} > 160$ and 190 for events with an L1 threshold of 40 GeV. While all events with $N_{\mathrm{trk}}^{\mathrm{online}} > 190$ are accepted, only a fraction of the events from the other thresholds are retained. This fraction is dependent on the instantaneous luminosity. Data from both the minimum-bias trigger and the high-multiplicity trigger are retained for offline analysis. Similar high-multiplicity triggers, with different thresholds, were developed for pp collisions, with details given in Ref. [8].

In the subsequent analysis of all collision systems, hadronic events are selected by requiring the presence of at least one energy deposit larger than 3 GeV in each of the two HF calorimeters. Events are also required to contain a primary vertex within 15 cm of the nominal interaction point along the beam axis and 0.15 cm in the transverse direction, where the primary vertex is the reconstructed vertex with the largest track multiplicity. At least two reconstructed tracks are required to be associated with this primary vertex, a condition that is important only for minimum-bias events. Beam-related background is suppressed by rejecting events in which less than 25% of all reconstructed tracks satisfy the high-purity selection defined in Ref. [38]. In the pPb data sample, there is a 3% probability to have at least one additional interaction in the same bunch crossing (pileup). The procedure used to reject pileup events in pPb collisions is described in Ref. [41]. It is based on the number of tracks associated with each reconstructed vertex and the distance between different vertices. A purity of 99.8% for single pPb collision events is achieved for the highest multiplicity pPb range studied in this Letter. For the pp data, the average number of collisions per bunch crossing is 1.2. However, pp interactions that are

well separated from each other do not interfere. Thus, among events identified as containing pileup, the event is retained if the separation between the primary vertex and any other vertex exceeds 1 cm. In such events, only tracks from the highest multiplicity vertex are used.

With the above criteria, 97% (98%) of the simulated pPb events generated with the EPOS LHC [44] (HIJING 2.1 [45]) programs are selected. Similarly, 94% (96%) of the pp events simulated with the PYTHIA 6 Tune Z2 [46] (PYTHIA 8 Tune 4C [47]) programs are selected.

The event-by-event charged-particle multiplicity $N_{\mathrm{trk}}^{\mathrm{offline}}$ is defined using primary tracks, i.e, tracks that satisfy the high-purity criteria of Ref. [38] and, in addition, the following criteria designed to improve track quality and ensure the tracks emanate from the primary vertex. The impact parameter significance of the track with respect to the primary vertex in the direction along the beam axis, $d_z/\sigma(d_z)$, is required to be less than 3, as is the corresponding impact parameter in the transverse plane, $d_T/\sigma(d_T)$. The relative p_T uncertainty, $\sigma(p_T)/p_T$, must be less than 10%. To ensure high tracking efficiency and to reduce the rate of misreconstructed tracks, the tracks are required to satisfy $|\eta| < 2.4$ and $p_T > 0.4\,\mathrm{GeV}$. Based on simulated samples generated with the HIJING program, the efficiency for primary track reconstruction is found to be greater than 80% for charged particles with $p_T > 0.6\,\mathrm{GeV}$ and $|\eta| < 2.4$. For the multiplicity range studied in this Letter, no dependence of the tracking efficiency on multiplicity is found and the rate of misreconstructed tracks is 1–2%.

The pp, pPb, and PbPb data are divided into classes based on $N_{\mathrm{trk}}^{\mathrm{offline}}$. The quantity $N_{\mathrm{trk}}^{\mathrm{corrected}}$ is the corresponding multiplicity corrected for detector and algorithm inefficiencies in the same kinematic region ($|\eta| < 2.4$ and $p_T > 0.4\,\mathrm{GeV}$). The fraction of the total multiplicity found in each interval and the average number of tracks both before and after accounting for the corrections are listed in Table 1 for the pp data and in Ref. [41] for the pPb and PbPb data. The uncertainty in the average value $\langle N_{\mathrm{trk}}^{\mathrm{corrected}}\rangle$ is evaluated from the uncertainty in the tracking efficiency, which is 3.9% for a single track [48]. For the pp data, six multiplicity intervals, indicated in Table 1, are defined, which are inclusive for the lower bounds and exclusive for the upper bounds, as indicated in Table 1. The average $N_{\mathrm{trk}}^{\mathrm{offline}}$ value of minimum-bias events is similar to that for the multiplicity range $N_{\mathrm{trk}}^{\mathrm{offline}} < 35$. For the pPb and PbPb data, eight intervals are defined. These eight intervals are indicated, e.g., in the legend of Fig. 2. Note that, unlike pp and PbPb collisions, $N_{\mathrm{trk}}^{\mathrm{offline}}$ for pPb collisions is not determined in the center-of-mass frame. However, the difference in the $N_{\mathrm{trk}}^{\mathrm{offline}}$ definition between the laboratory and the center-of-mass frames is found to be minimal and so this difference is ignored. The detector condition has been checked to be stable for events with different multiplicities.

Table 1: Fraction of the full event sample in each multiplicity interval and the average multiplicity per interval for pp data. The multiplicities $N_{\mathrm{trk}}^{\mathrm{offline}}$ and $N_{\mathrm{trk}}^{\mathrm{corrected}}$ are determined for $|\eta| < 2.4$ and $p_T > 0.4\,\mathrm{GeV}$ before and after efficiency corrections, respectively. The third and fourth columns list the average values of $N_{\mathrm{trk}}^{\mathrm{offline}}$ and $N_{\mathrm{trk}}^{\mathrm{corrected}}$.

Multiplicity interval ($N_{\mathrm{trk}}^{\mathrm{offline}}$)	Fraction	$\langle N_{\mathrm{trk}}^{\mathrm{offline}}\rangle$	$\langle N_{\mathrm{trk}}^{\mathrm{corrected}}\rangle$
$[0, 35)$	0.93	12	14 ± 1
$[35, 60)$	0.06	43	50 ± 2
$[60, 90)$	6×10^{-3}	68	79 ± 3
$[90, 110)$	2×10^{-4}	97	112 ± 4
$[110, 130)$	1×10^{-5}	116	135 ± 5
$[130, \infty)$	7×10^{-7}	137	158 ± 6

4 The K^0_S, Λ, and Ξ^- reconstruction and yields

The reconstruction and selection procedures for K^0_S, Λ, and Ξ^- candidates are presented in Refs. [30, 49]. To increase the efficiency for tracks with low momenta and large impact parameters, both characteristic of the strange-particle decay products, the loose selection of tracks, as defined in Ref. [38], is used. The K^0_S and Λ candidates (generically referred to as "V^0s") are reconstructed, by combining oppositely charged particles to define a secondary vertex. Each of the two tracks must have hits in at least four layers of the silicon tracker, and transverse and longitudinal impact parameter significances with respect to the primary vertex greater than 1. The distance of closest approach of the pair of tracks to each other is required to be less than 0.5 cm. The fitted three-dimensional vertex of the pair of tracks is required to have a χ^2 value divided by the number of degrees of freedom less than 7. Each of the two tracks is assumed to be a pion in the case of the K^0_S reconstruction. As the proton carries nearly all of the momentum in the Λ decay, the higher-momentum track is assumed to be a proton and the other track a pion in the case of the Λ reconstruction. To reconstruct Ξ^- particles, a Λ candidate is combined with an additional charged particle carrying the correct sign, to define a common secondary vertex. This additional track is required to have hits in at least four layers of the silicon tracker, and both the transverse and longitudinal impact parameter significances with respect to the primary vertex are required to exceed 3.
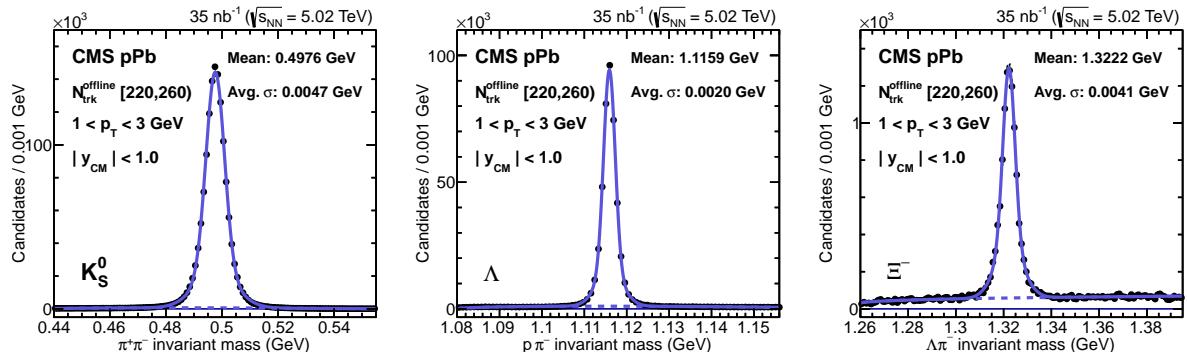

Figure 1: Invariant mass distribution of K^0_S (left), Λ (middle), and Ξ^- (right) candidates in the p_T range 1–3 GeV for $220 \leq N^{\mathrm{offline}}_{\mathrm{trk}} < 260$ in pPb collisions. The inclusion of the charge-conjugate states is implied for Λ and Ξ^- particles. The solid lines show the results of fits described in the text. The dashed lines indicate the fitted background component.

Due to the long lifetime of the K^0_S and Λ particles, the significance of the V^0 decay length, which is the three-dimensional distance between the primary and V^0 vertices divided by its uncertainty, is required to exceed 5. To remove K^0_S candidates misidentified as Λ particles and vice versa, the Λ (K^0_S) candidate mass assuming both tracks to be pions (the lower-momentum track to be a pion and the higher-momentum track a proton) must differ by more than 20 (10) MeV from the nominal [50] K^0_S (Λ) mass value. To remove photon conversions to an electron-positron pair, the mass of a K^0_S or Λ candidate assuming both tracks to have the electron mass must exceed 15 MeV. The angle θ^{point} between the V^0 momentum vector and the vector connecting the primary and V^0 vertices is required to satisfy $\cos\theta^{\mathrm{point}} > 0.999$. This reduces the contributions of particles from nuclear interactions, random combinations of tracks, and secondary Λ particles originating from the weak decays of Ξ and Ω particles.

To optimize the reconstruction of Ξ^- particles, requirements on the three-dimensional impact parameter significance of its decay products with respect to the primary vertex are applied. This significance must be larger than 3 (4) for the proton (pion) tracks from the Λ decay, and larger than 5 for the direct pion candidate from the Ξ^- decay. To further reduce the background

from random combinations of tracks, the corresponding impact parameter significance of Ξ^- candidates cannot exceed 2.5. The three-dimensional decay length significance, with respect to the primary vertex, of the Ξ^- candidate and the associated Λ candidate must exceed 3 and 12, respectively.

The K_S^0, Λ, and Ξ^- reconstruction efficiencies are about 15, 5, and 0.7% for $p_T \approx 1\,\text{GeV}$, and 20, 10, and 2% for $p_T > 3\,\text{GeV}$, averaged over $|\eta| < 2.4$. These efficiencies account for the effects of acceptance, and for the branching fractions of the decay modes in which the strange particles are reconstructed. The invariant mass distributions of reconstructed K_S^0, Λ, and Ξ^- candidates with $1 < p_T < 3\,\text{GeV}$ are shown in Fig. 1 for pPb events with $220 \leq N_{\text{trk}}^{\text{offline}} < 260$. Prominent mass peaks are visible, with little background. The solid lines show the result of a maximum likelihood fit. In this fit, the strange-particle peaks are modeled as the sum of two Gaussian functions with a common mean. The "average σ" values in Fig. 1 are the square root of the weighted average of the variances of the two Gaussian functions. The background is modeled with a quadratic function for the K_S^0 results, with the analytic form $Aq^{1/2} + Bq^{3/2}$ with $q = m - (m_\pi + m_p)$ for the Λ results, and with the form Cq^D with $q = m - (m_\Lambda + m_\pi)$ for the Ξ^- results, where A, B, C, and D are fitted parameters. These fit functions are found to provide a good description of the signal and background with relatively few free parameters. The fits are performed over the ranges of strange-particle invariant masses indicated in Fig. 1 to obtain the raw strange-particle yields $N_{K_S^0/\Lambda/\Xi^-}^{\text{raw}}$.

The raw strange-particle yields are corrected to account for the branching fraction of the reconstructed decay mode, and for the acceptance and reconstruction efficiency of the strange particle, using simulated event samples based on the PYTHIA 6 (pp) or EPOS (pPb and PbPb) event generator and GEANT4 modeling of the detector:

$$N_{K_S^0/\Lambda/\Xi^-}^{\text{corr}} = \frac{N_{K_S^0/\Lambda/\Xi^-}^{\text{raw}}}{R_{\text{corr}}}, \tag{1}$$

where R_{corr} is a correction factor from simulation given by the ratio of the raw reconstructed yield to the total generated yield for the respective strange particle, with $N_{K_S^0/\Lambda/\Xi^-}^{\text{corr}}$ the corrected yield.

The raw Λ particle yield includes contributions from the decays of Ξ^- and Ω particles. This "nonprompt" contribution is largely determined by the relative Ξ^- to Λ yield (because the contribution from Ω particles is negligible). The stringent requirements placed on $\cos\theta^{\text{point}}$ remove a large fraction of the nonprompt Λ component but, from simulation, up to 10% of the Λ candidates at high p_T are nonprompt. If the relative Ξ^- to Λ yield in simulation is modeled precisely, the contamination from nonprompt Λ particles will be removed by the correction procedure of Eq. (1). Otherwise, an additional correction to account for the residual contamination is necessary. As the Ξ^- particle yields are explicitly measured in this analysis, this residual correction factor can be determined directly from the data as:

$$f_{\Lambda,\text{np}}^{\text{residual}} = 1 + f_{\Lambda,\text{np}}^{\text{raw,MC}} \left(\frac{N_{\Xi^-}^{\text{corr}} / N_{\Lambda}^{\text{corr}}}{N_{\Xi^-}^{\text{MC}} / N_{\Lambda}^{\text{MC}}} - 1 \right), \tag{2}$$

where $f_{\Lambda,\text{np}}^{\text{raw,MC}}$ denotes the fraction of nonprompt Λ particles in the raw reconstructed Λ sample as determined from simulation, while $N_{\Xi^-}^{\text{corr}} / N_{\Lambda}^{\text{corr}}$ and $N_{\Xi^-}^{\text{MC}} / N_{\Lambda}^{\text{MC}}$ are the Ξ^--to-Λ yield ratios from the data after applying the corrections of Eq. (1), and from generator-level simulation, respectively. The final prompt Λ particle yield is given by $N_{\Lambda}^{\text{corr}} / f_{\Lambda,\text{np}}^{\text{residual}}$. Based on EPOS MC studies, which has a similar Ξ^-/Λ ratio to the data, the residual nonprompt contributions to

the Λ yields are found to be negligible in pPb and PbPb collisions, while in pp collisions the correction is 1–3% depending on the p_T value of the Λ particle. Note that N_Λ^{corr} in Eq. (2) is derived using Eq. (1), which in principle contains the residual nonprompt Λ contributions. Nonetheless, by applying Eq. (2) in an iterative fashion, we expect N_Λ^{corr} to approach a result corresponding to prompt Λ particles only. A second iteration of correction is found to have an effect of less than 0.1% on the Λ particle yield. As a cross-check we treat the sample of simulated events generated with the HIJING program like data and verify that we obtain the correct yields at the generator level after applying the correction procedure described above.

5 Systematic uncertainties

Table 2 summarizes the different sources of systematic uncertainty in the yields of each strange particle species. The values in parentheses correspond to the systematic uncertainties in the forward rapidity regions ($-2.4 < y_{cm} < -1.5$ and $0.8 < y_{cm} < 1.5$) for pPb data, if they differ from those at mid-rapidity. The dominant sources of systematic uncertainty are associated with the strange-particle reconstruction, especially the efficiency determination.

Table 2: Summary of systematic uncertainties for the p_T spectra of K_S^0, Λ, and Ξ^- particles in the center-of-mass rapidity range $|y_{cm}| < 1.0$ (for pPb events, at forward rapidities, if different) for the three collision systems.

Source	K_S^0 (%)		Λ (%)		Ξ^- (%)
p_T (GeV)	<1.5	>1.5	<1.5	>1.5	
Single-track efficiency	7.8	7.8	7.8	7.8	11.7
Yield extraction	2 (3)	2 (3)	2 (4)	2 (4)	3
Selection criteria	3.6 (3.6)	2.2 (3.6)	3.6 (6.4)	2.2 (6.4)	7
Momentum resolution	2	2	2	2	2
Nonprompt Λ correction			2	2	
Pileup (pp only)	3	1	3	1	3
Proton direction (pPb only)	3 (3)	3 (3)	3 (5)	3 (5)	4
Rapidity binning	1 (2)	1 (2)	1 (3)	1 (3)	2
Efficiency correction					5
Total (pp)	9.6	8.7	9.8	8.9	15.4
Total (pPb)	9.6 (10.0)	9.2 (10.0)	9.8 (12.6)	9.4 (12.6)	15.6
Total (PbPb)	9.1	8.6	9.3	8.9	15.1

The systematic uncertainty in determining the efficiency of a single track is 3.9% [48]. The tracking efficiency is strongly correlated with the lifetime of a particle because when and where a particle decays determine how efficiently the detector captures its decay products. We observe agreement of the K_S^0 lifetime distribution ($c\tau$) between data and simulation, and similarly for the Λ and Ξ^-, which provides a cross-check of the systematic uncertainty. This translates into a systematic uncertainty in the reconstruction efficiency of 7.8% for the K_S^0 and Λ particles, and 11.7% for the Ξ^- particles. Different background fit functions and methods to extract the yields for the K_S^0, Λ, and Ξ^- are compared. The background fit function is varied to a fourth-order polynomial for the K_S^0 and Λ studies, and to a linear function for the Ξ^- study. The yields are obtained by integrating over a region that is ± 5 times the average resolution and centered at the mean, rather than over the entire fitted mass range. Possible contamination by residual misidentified V^0 candidates (i.e., a K_S^0 particle misidentified as a Λ particle, or vice versa) is investigated by varying the invariant mass range used to reject misidentified V^0 candidates. On the basis of these studies we assign systematic uncertainties of 2–4% to the yields. Systematic

effects related to the selection of the strange-particle candidates are evaluated by varying the selection criteria, resulting in an uncertainty of 1–7%. The impact of finite momentum resolution on the spectra is estimated using the EPOS event generator. Specifically, the generator-level p_T spectra of the strange particles are smeared by the momentum resolution, which is determined through comparison of the generator-level and matched reconstructed-level particle information. The difference between the smeared and original spectra is less than 2%. The systematic uncertainty associated with nonprompt Λ corrections to the Λ spectra is evaluated through propagation of the systematic uncertainty in the $N_{\Xi^-}^{\rm corr} / N_\Lambda^{\rm corr}$ ratio in Eq. (2) to the $f_{\Lambda, \rm np}^{\rm residual}$ factor, and is found to be less than 2%. Systematic uncertainties introduced by possible residual pileup effects for pp data are estimated to be 1–3%. This uncertainty is evaluated through both tightening (only one reconstructed vertex allowed per event) and loosening (no event rejection on the basis of the number of vertices) the pileup rejection criteria [41]. The uncertainty associated with pileup is negligible for the pPb and PbPb data since there are very few events in those samples with more than one reconstructed vertex. In pPb collisions, the direction of the p and Pb beams were reversed during course of the data collection, as mentioned in Section 2. Comparison of the particle p_T spectra with and without the beam reversal yields an uncertainty of 2–5% for all particle types. The effect of the choice of the rapidity bins is assessed by dividing each bin into two, thereby doubling the number of bins, resulting in a systematic uncertainty of 1–3% for the p_T spectra. For the Ξ^-, the reconstruction efficiency correction is smoothed by averaging adjacent bins in order to compensate for the limited statistical precision of the MC sample. Variations in the smoothing procedure lead to a systematic uncertainty of 5% for the p_T spectra of the Ξ^-.

All sources of systematic uncertainty are uncorrelated and summed in quadrature to define the total systematic uncertainties in the p_T spectra of each strange particle. The total systematic uncertainties between the pp, pPb, and PbPb systems are similar and largely correlated. When calculating ratios of particle yields, most of the systematic uncertainties partially or entirely cancel. For example, the systematic uncertainties due to tracking efficiency and pileup for the $\Lambda/2{\rm K}_{\rm S}^0$ ratio are negligible.

6   Results

6.1   Multiplicity dependence at mid-rapidity

The p_T spectra of ${\rm K}_{\rm S}^0$, Λ, and Ξ^- particles with $|y_{\rm cm}| < 1$ in pp collisions at $\sqrt{s} = 7\,{\rm TeV}$ (top), pPb collisions at $\sqrt{s} = 5.02\,{\rm TeV}$ (middle), and PbPb collisions at $\sqrt{s_{NN}} = 2.76\,{\rm TeV}$ (bottom) are presented in Fig. 2, for different multiplicity intervals. Due to details in the implementation of the dedicated high-multiplicity trigger thresholds used to select the pp events, the multiplicity intervals for pp events differ slightly from those for pPb and PbPb events. The p_T differential yield is defined as $dN^2/(2\pi p_T)dp_T\,dy$. For the purpose of better visibility, the data are scaled by factors of 2^{-n}, as indicated in the figure legend. A clear evolution of the spectral shape with multiplicity can be seen for each particle species in each collision system. For higher multiplicity events, the spectra tend to become flatter (i.e., "harder"), indicating a larger $\langle {\rm KE}_T \rangle$ value. Within each collision system, heavier particles (e.g., Ξ^-) exhibit a harder spectrum than lighter particles (${\rm K}_{\rm S}^0$), especially for high-multiplicity events.

To examine the differences in the multiplicity dependence of the spectra in greater detail, the ratios $\Lambda/2{\rm K}_{\rm S}^0$ and Ξ^-/Λ of the yields are shown in Fig. 3 as a function of p_T for different multiplicity ranges in the pp, pPb, and PbPb systems. The results for the $\Lambda/2{\rm K}_{\rm S}^0$ ratio are shown in Fig. 3 (top). For $p_T \lesssim 2\,{\rm GeV}$, the $\Lambda/2{\rm K}_{\rm S}^0$ ratio is seen to be smaller in high-multiplicity events
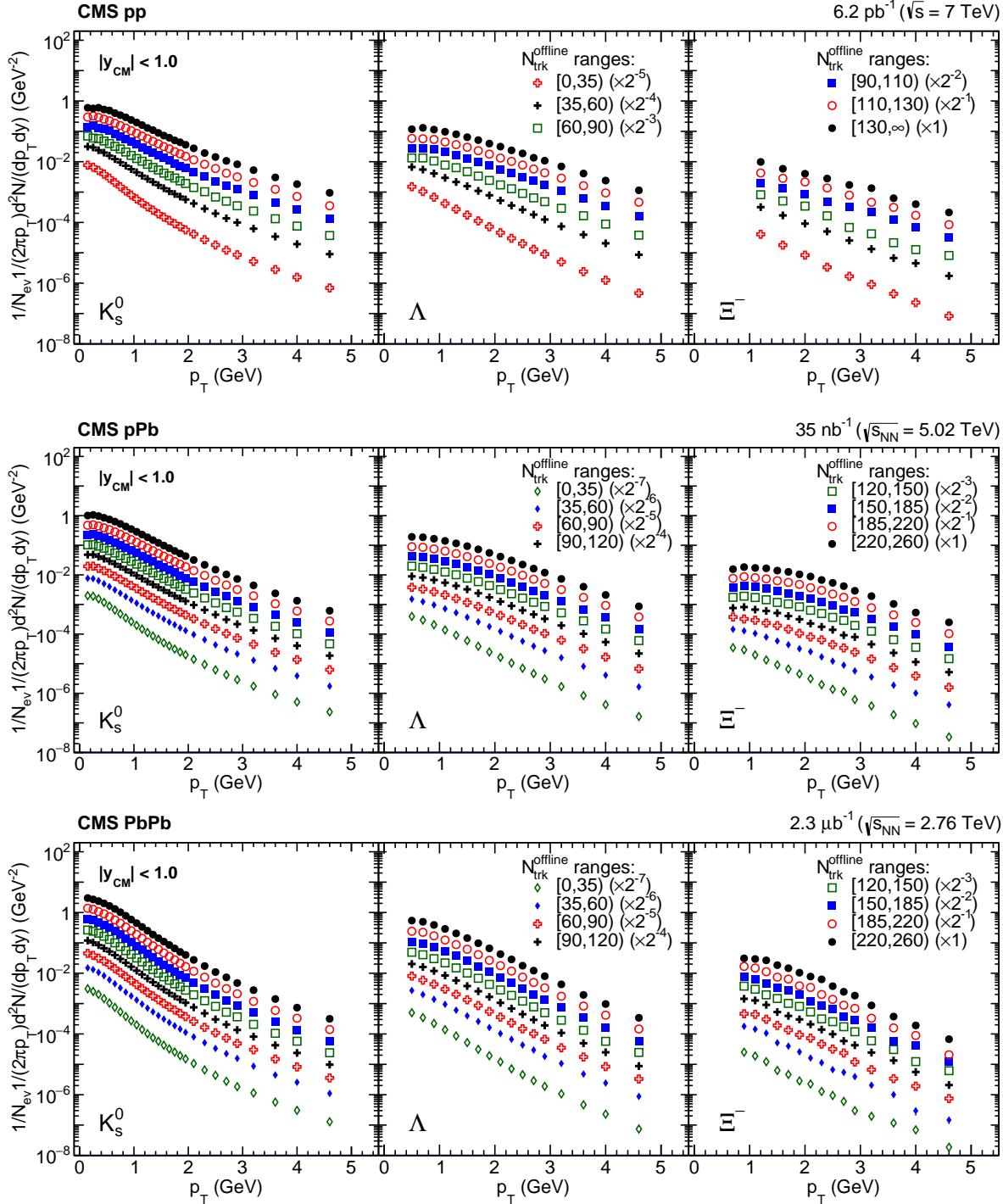
Figure 2: The p_T spectra of K_S^0, Λ, and Ξ^- particles in the center-of-mass rapidity range $|y_{cm}| < 1$ in pp collisions at $\sqrt{s} = 7$ TeV (top), pPb collisions at $\sqrt{s} = 5.02$ TeV (middle), and PbPb collisions at $\sqrt{s_{NN}} = 2.76$ TeV (bottom) for different multiplicity intervals. The inclusion of the charge-conjugate states is implied for Λ and Ξ^- particles. The data in the different multiplicity intervals are scaled by factors of 2^{-n} for better visibility. The statistical uncertainties are smaller than the markers and the systematic uncertainties are not shown.
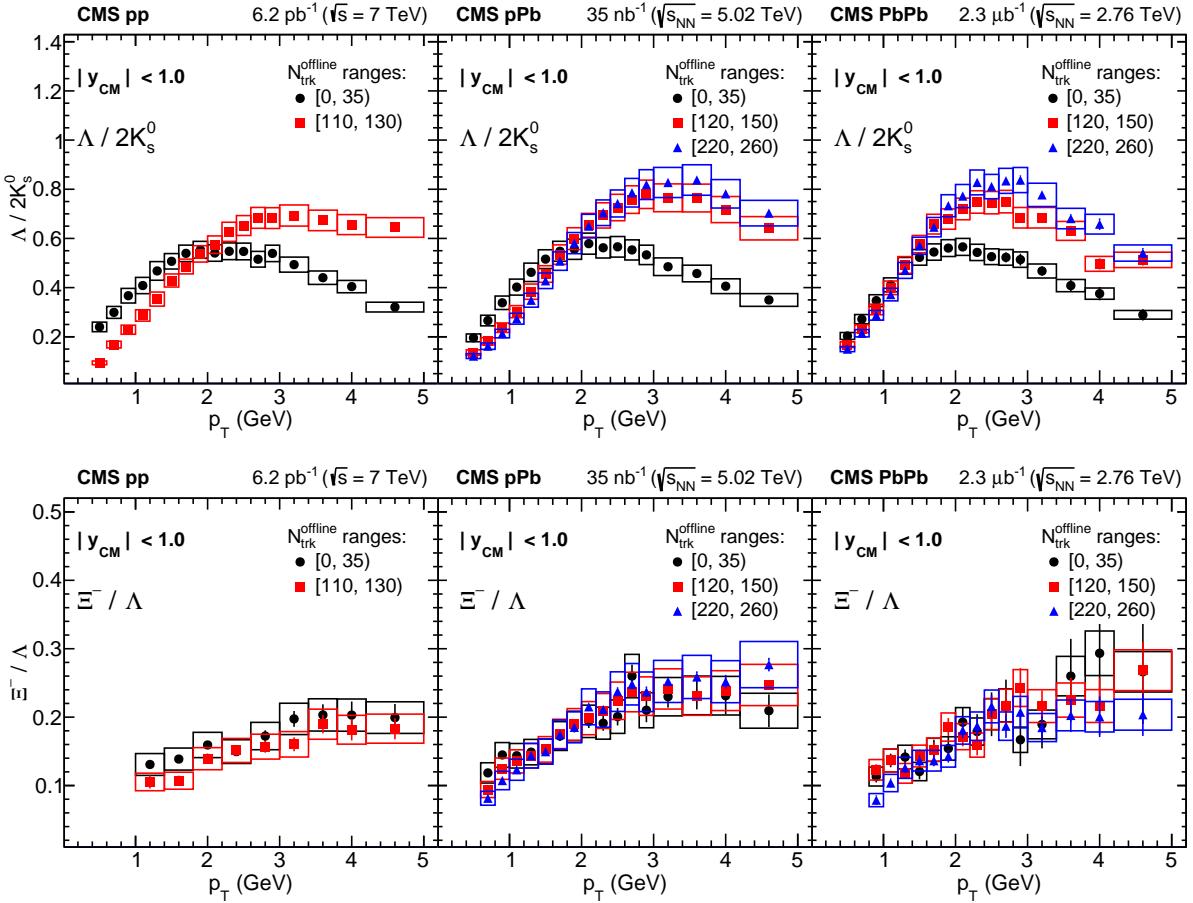
Figure 3: Ratios of p_T spectra for $\Lambda/2K_S^0$ (top) and Ξ^-/Λ (bottom) in the center-of-mass rapidity range $|y_{cm}| < 1.0$ for pp collisions at $\sqrt{s} = 7\,\text{TeV}$ (left), pPb collisions at $\sqrt{s} = 5.02\,\text{TeV}$ (middle), and PbPb collisions at $\sqrt{s_{NN}} = 2.76\,\text{TeV}$ (right). Two (for pp) or three (for pPb and PbPb) representative multiplicity intervals are presented. The inclusion of the charge-conjugate states is implied for Λ and Ξ^- particles. The error bars represent the statistical uncertainties, while the boxes indicate the systematic uncertainties.

than in low-multiplicity events for a given p_T value. In pp and pPb collisions, this trend is similar to what has been observed between peripheral and central PbPb collisions [23]; this trend is not as evident for the PbPb data in Fig. 3 (top right) because in the present study only PbPb events of 50–100% centrality are considered. At higher p_T, this multiplicity ordering of the $\Lambda/2K_S^0$ ratio is reversed. In hydrodynamic models such as those presented in Refs. [51, 52], this behavior can be interpreted as the effect of radial flow. A stronger radial flow is developed in higher-multiplicity events, which boosts heavier particles (e.g., Λ) to higher p_T, resulting in a suppression of the $\Lambda/2K_S^0$ ratio at low p_T. Comparing the various collision systems at low p_T, the difference in the $\Lambda/2K_S^0$ ratio between low- and high-multiplicity events is seen to be largest for the pp data. In the hydrodynamic model of Ref. [31], smaller collision systems like pp produce a larger radial-flow effect than larger systems like pPb or PbPb, for similar multiplicities, which could explain this observation. For $p_T > 2\,\text{GeV}$, the baryon enhancement could be explained by recombination models, in which free quarks recombine to form hadrons [53]. In previous studies (e.g., Ref. [54]), it has been shown that the average p_T value of various particle species has only a slight center-of-mass energy dependence (10% at high multiplicity). This dependence is not sufficient to explain the differences observed in Fig. 3 between the various

systems.

For each multiplicity interval, the $\Lambda/2K_S^0$ ratio reaches a maximum that has a similar value for all three collision processes, and then decreases at higher p_T. The location of the maximum increases with multiplicity from around $p_T = 2$ to $3\,\text{GeV}$.

The results for the Ξ^-/Λ ratio are shown in Fig. 3 (bottom). In this case, the difference between the low- and high-multiplicity events is much smaller than for the $\Lambda/2K_S^0$ ratio, for all three collisions systems. For all systems, the Ξ^-/Λ ratio increases with p_T and reaches a plateau at around $p_T = 3\,\text{GeV}$. Due to the large systematic uncertainty, it is not possible to draw a conclusion with respect to the radial-flow interpretation.
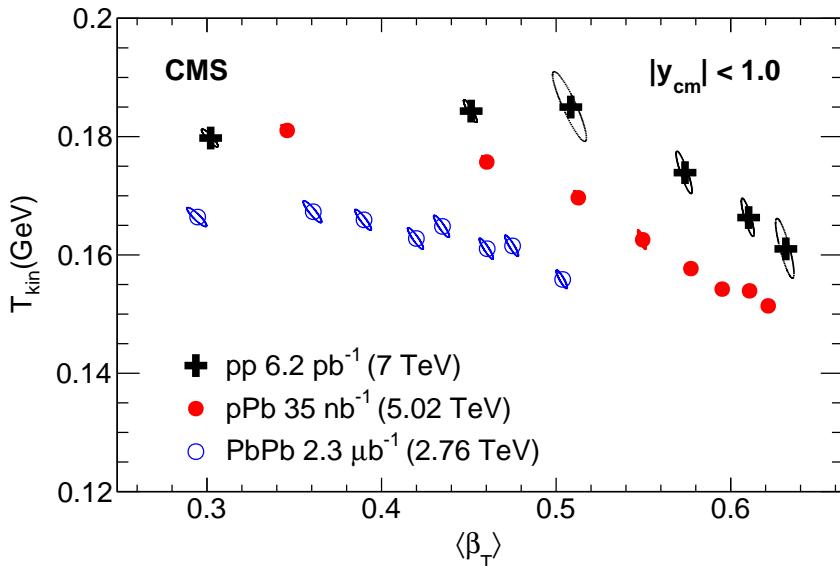
Figure 4: The extracted kinetic freeze-out temperature, T_{kin}, versus the average radial-flow velocity, $\langle \beta_T \rangle$, from a simultaneous blast-wave fit to the K_S^0 and Λ p_T spectra at $|y_{cm}| < 1$ for different multiplicity intervals in pp, pPb, and PbPb collisions. The six pp and eight pPb and PbPb multiplicity intervals are indicated in the legend of Fig. 2. For the results in this plot, the multiplicity increases from left to right. The correlation ellipses represent the statistical uncertainties. Systematic uncertainties, which are evaluated to be on the order of a few percent, are not shown.

Motivated by the hydrodynamic model, we perform a simultaneous fit of a blast-wave function [32] to the K_S^0 and Λ spectra in Fig. 2. The fits are restricted to low p_T because that is the region in which the blast-wave model is valid. The blast-wave model is strictly appropriate only for directly produced particles, while about $1/3$ of the K_S^0 mesons may be from higher mass resonances [55]. The Ξ^- particle is not used in the fit as there are not many Ξ^- at low p_T. The fits are performed for each collision system separately. The fit ranges are $0.1 < p_T < 1.5\,\text{GeV}$ for the K_S^0 and $0.6 < p_T < 3.0\,\text{GeV}$ for the Λ. The fitted function is:

$$\frac{1}{p_T}\frac{dN}{dp_T} \sim \int_0^R r\,dr\,m_T I_0\left(\frac{p_T \sinh\rho}{T_{kin}}\right) K_1\left(\frac{m_T \cosh\rho}{T_{kin}}\right),\tag{3}$$

where $\rho = \tanh^{-1}\beta_T = \tanh^{-1}\left(\beta_s(r/R)^n\right)$ is the velocity profile, R is the radius of the medium (set to unity in the fit), r is the radial distance from the center of the medium in the transverse plane, n is the exponent of the velocity profile, β_T is the transverse expansion velocity (also

known as the radial-flow velocity), β_s is the transverse expansion velocity on the surface of the medium, T_{kin} is the kinetic freeze-out temperature, and I_0 and K_1 are modified Bessel functions. The fitted parameters that govern the shape are n, β_s, and T_{kin}.

In the blast-wave model, common values of T_{kin} and average radial-flow velocity $\langle \beta_T \rangle$ are assumed for all particle species, as is expected if the system is locally thermalized and undergoes a radial-flow expansion. It is useful to directly compare the extracted values of T_{kin} and $\langle \beta_T \rangle$ from the different systems to study the system-size dependence at similar multiplicities.
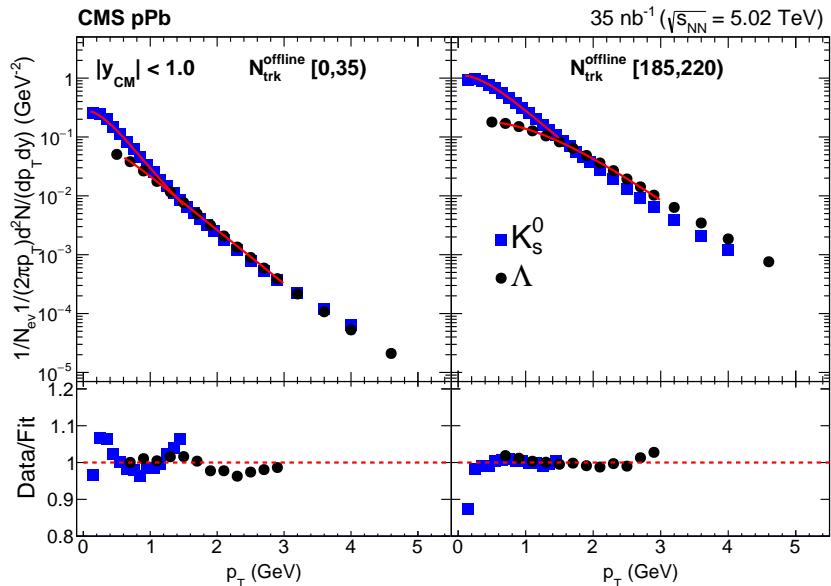
Figure 5: Examples of simultaneous blast-wave fits of the p_T spectra of K_S^0 and Λ particles in low- and high-multiplicity pPb events. The inclusion of the charge-conjugate states is implied for Λ particles. The ratios of the fits to the data as a function of p_T are shown in the bottom panels. The uncertainties are statistical only and are too small to be visible for most of the points.

The extracted values of T_{kin} and $\langle \beta_T \rangle$ are shown in Fig. 4 for the six pp and for the eight pPb and PbPb multiplicity intervals. In this figure, the multiplicity increases from left to right. The ellipses correspond to one standard deviation statistical uncertainties, which for pp collisions are smaller at low and high multiplicity due to the use of events collected with minimum bias and high-multiplicity triggers. Systematic uncertainties, which are evaluated by propagating the systematic uncertainties from the spectra to the blast-wave fits and altering the fit ranges, are on the order of a few percent and are not shown. Examples of the fits are shown in Fig. 5 for a low- and high-multiplicity range in pPb collisions. In general, the fit quality is good for high-multiplicity events except for the lowest p_T range, while for low-multiplicity events there are discrepancies on the order of 5%. However, the discrepancies between the fit and data lie within the systematic uncertainty.

The precise meaning of the T_{kin} and $\langle \beta_T \rangle$ parameters is model dependent, and they should not be interpreted literally as the kinetic freeze-out temperature and radial-flow velocity of the system. The main purpose of Fig. 4 is to provide a qualitative comparison of the spectral shapes in the three systems. In the context of the blast-wave model, when comparing at similar multiplicities, the T_{kin} parameter has the same value within 15% among the three systems, while the $\langle \beta_T \rangle$ parameter is larger when the system is smaller, i.e., $\langle \beta_T \rangle_{pp} > \langle \beta_T \rangle_{pPb} > \langle \beta_T \rangle_{PbPb}$. This is qualitatively consistent with the prediction of Ref. [31]. The results of blast-wave fits are known to depend on the particle species. Due to the limited set of particles in this analysis,

future studies will be needed to further substantiate the conclusions.
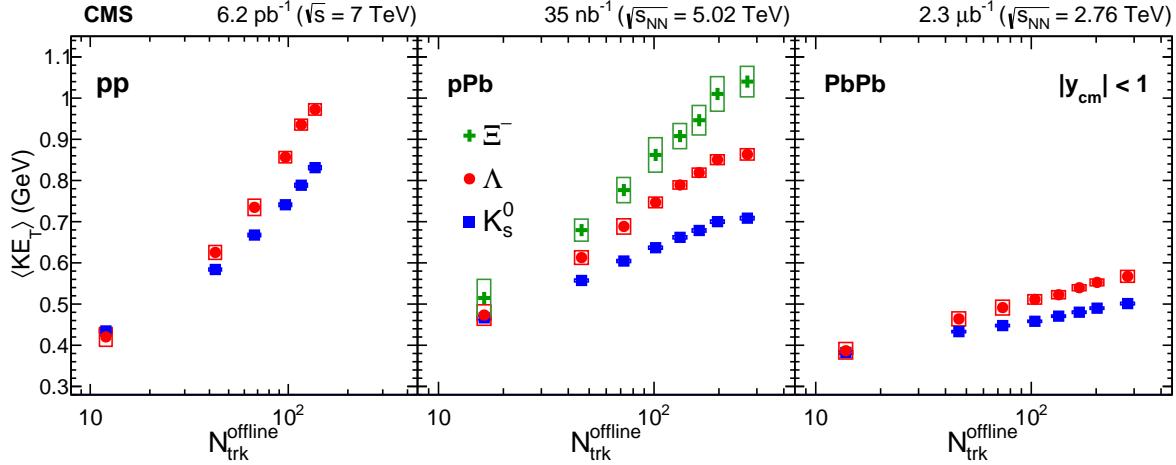

Figure 6: The average transverse kinetic energy, $\langle KE_T \rangle$, at $|y_{cm}| < 1$ for K_S^0, Λ, and Ξ^- particles as a function of multiplicity in pp, pPb, and PbPb collisions. The inclusion of the charge-conjugate states is implied for Λ and Ξ^- particles. For the Ξ^-, only results from pPb collisions are shown. The error bars represent the statistical uncertainties, while the boxes indicate the systematic uncertainties.

The evolution of the p_T spectra with multiplicity can be compared more directly between the three systems through examination of the $\langle KE_T \rangle$ value. The $\langle KE_T \rangle$ values at $|y_{cm}| < 1$ for K_S^0, Λ, and Ξ^- particles as a function of multiplicity are shown in Fig. 6. Extrapolation of the p_T spectra down to $p_T = 0$ GeV is a crucial step in extracting the $\langle KE_T \rangle$ values, while the impact of the extrapolation up to $p_T \approx \infty$ is negligible, both on the value of $\langle KE_T \rangle$ and its uncertainty. For the Ξ^- particle, only results in pPb collisions are shown due to the limitation of the low-p_T reach in pp and PbPb collisions, as can be seen from Fig. 2. Blast-wave fits to the individual spectra, which only consider the spectrum shape but do not impose any physics constraint, are used to obtain the extrapolation. The fraction of the extrapolated yield with respect to the total yield is about 1.2–2.5% for the K_S^0, 5.8–15.1% for the Λ, and 5.4–20.4% for the Ξ^- particles, depending on the multiplicity. Alternative methods to perform the extrapolation are used to evaluate a systematic uncertainty, including use of the predictions from the simultaneous blast-wave fit to the K_S^0 and Λ p_T spectra, and a linear extrapolation from the yields in a low range of p_T. The systematic uncertainties from Table 2 are also included in the evaluation of the $\langle KE_T \rangle$ uncertainties.

For the lowest multiplicity range, the $\langle KE_T \rangle$ values for each particle species are seen to be similar. For all particle species, $\langle KE_T \rangle$ increases with increasing multiplicity. However, the slope of the increase differs for different particles, with the heavier particles exhibiting a faster growth in $\langle KE_T \rangle$ for all systems. For a given multiplicity range, the $\langle KE_T \rangle$ value is roughly proportional to the particle's mass. In PbPb collisions, this can be understood to be due to the onset of radial flow [2, 7]. The observed difference between particle species at high multiplicity is seen to be larger for pp and pPb events than for PbPb events. Note, however, the difference in the center-of-mass energies between the three systems.

6.2   Rapidity dependence in pPb events

The rapidity dependence of the p_T spectra of the K_S^0 and Λ particles is studied in the pPb data. No results for Ξ^- particles are presented due to statistical limitations. As a pPb collision is asymmetric in rapidity, it is interesting to compare the spectra along the Pb-going ($y_{cm} < 0$)
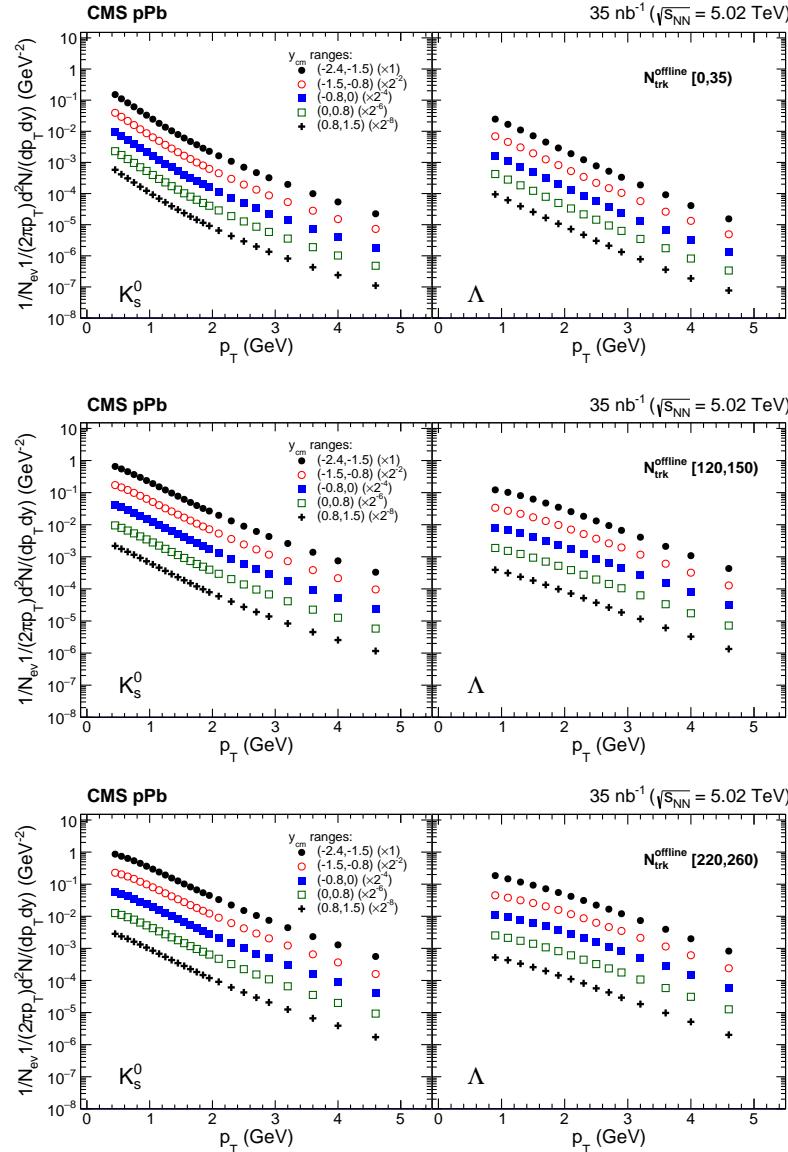
Figure 7: The p_T spectra of K_S^0 and Λ particles in different y_{cm} ranges for pPb collisions at $\sqrt{s} =$ 5.02 TeV. The inclusion of the charge-conjugate states is implied for Λ and particles. Results are shown for three multiplicity ranges: $0 \leq N_{trk}^{offline} < 35$ (top), $120 \leq N_{trk}^{offline} < 150$ (middle), and $220 \leq N_{trk}^{offline} < 260$ (bottom). Within each panel, the curves on top represent Pb-going events and the curves on bottom p-going events. The data in the different rapidity intervals are scaled by factors of 2^{-2n} for better visibility. The statistical uncertainties are smaller than the markers and the systematic uncertainties are not shown.

and p-going ($y_{cm} > 0$) directions [37]. The p_T spectra of K_S^0 and Λ particles in different y_{cm} ranges are shown in Fig. 7 for small (top), intermediate (middle), and large (bottom) average multiplicities.
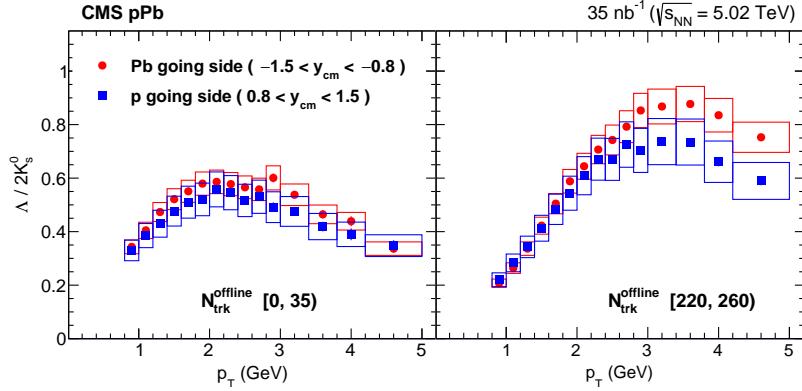
Figure 8: Ratios of p_T spectra, $\Lambda/2K_S^0$, from the $-1.5 < y_{cm} < -0.8$ (Pb-going) and $0.8 < y_{cm} < 1.5$ (p-going) rapidity regions in pPb collisions at $\sqrt{s} = 5.02\,\text{TeV}$. The inclusion of the charge-conjugate states is implied for Λ particles. Results are presented for two multiplicity ranges $0 \leq N_{trk}^{offline} < 35$ (left) and $220 \leq N_{trk}^{offline} < 260$ (right). The error bars represent the statistical uncertainties, while the boxes indicate the systematic uncertainties.

The $\Lambda/2K_S^0$ ratios from the $-1.5 < y_{cm} < -0.8$ (Pb-going) and $0.8 < y_{cm} < 1.5$ (p-going) rapidity regions are compared in Fig. 8 for multiplicity ranges $0 \leq N_{trk}^{offline} < 35$ and $220 \leq N_{trk}^{offline} < 260$. For both the low-multiplicity and the high-multiplicity events, the $\Lambda/2K_S^0$ ratio from the Pb-going direction lies above the results from the p-going direction, with the largest difference observed at high p_T in the high-multiplicity sample.
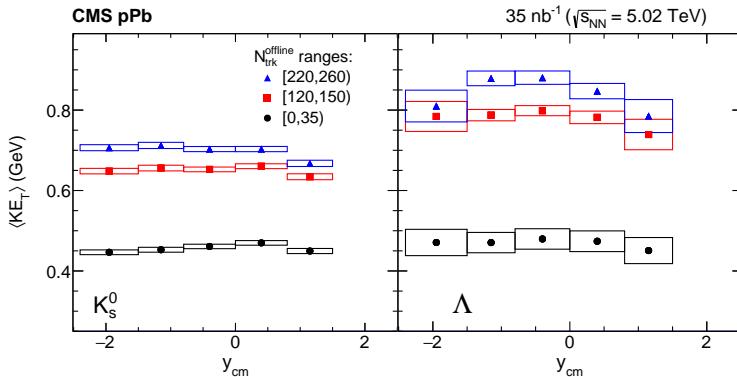

Figure 9: The average transverse kinetic energy, $\langle KE_T \rangle$, as a function of y_{cm} for the K_S^0 and Λ particles in three ranges of multiplicity in pPb collisions at $\sqrt{s} = 5.02\,\text{TeV}$. The inclusion of the charge-conjugate states is implied for Λ particles. The error bars represent the statistical uncertainties, while the boxes indicate the systematic uncertainties.

As a further study, we calculate $\langle KE_T \rangle$, following the procedure outlined in Section 6.1, and examine its dependence on y_{cm} for K_S^0 and Λ particles in the pPb collisions. The results are shown in Fig. 9. Although the systematic uncertainties at forward rapidities are large, the $\langle KE_T \rangle$ values are seen to become slightly asymmetric as multiplicity increases. At low multiplicities ($0 \leq N_{trk}^{offline} < 35$), the ratios of $\langle KE_T \rangle$ between the Pb-going side ($-1.5 < y_{cm} < -0.8$) and the p-going side ($0.8 < y_{cm} < 1.5$) are 1.01 ± 0.01 (syst.) for K_S^0 particles and 1.04 ± 0.05 (syst.) for Λ particles, both of which are consistent with unity within the systematic uncertainties

(the statistical uncertainties are negligible). However, in the highest multiplicity range, $220 \leq N_{\mathrm{trk}}^{\mathrm{offline}} < 260$, the ratios become 1.06 ± 0.01 (syst) for $\mathrm{K_S^0}$ particles and 1.12 ± 0.06 (syst) for Λ particles, suggesting that an asymmetry in $\langle \mathrm{KE_T} \rangle$ is developed between the Pb-going and p-going sides. This trend is qualitatively consistent with the hydrodynamic prediction for pPb collisions [37].

7   Summary

Measurements of strange hadron ($\mathrm{K_S^0}$, $\Lambda + \overline{\Lambda}$, and $\Xi^- + \overline{\Xi}^+$) transverse momentum spectra in pp, pPb, and PbPb collisions are presented over a wide range of event charged-particle multiplicity and particle rapidity. The study is based on samples of pp collisions at $\sqrt{s} = 7\,\mathrm{TeV}$, pPb collisions at $\sqrt{s} = 5.02\,\mathrm{TeV}$, and PbPb collisions at $\sqrt{s_{NN}} = 2.76\,\mathrm{TeV}$, collected with the CMS detector at the LHC. In the context of hydrodynamic models, the measured particle spectra are fitted with a blast wave function, which describes an expanding fluid-like system. When comparing at a similar multiplicity, the extracted radial-flow velocity parameters are found to be larger in pp and pPb collisions than that in PbPb collisions. The average transverse kinetic energy $\langle \mathrm{KE_T} \rangle$ of strange hadrons is observed to increase with multiplicity, with a stronger increase for heavier particles. At similar multiplicities, the difference in $\langle \mathrm{KE_T} \rangle$ between the strange-particle species is larger in the smaller pp and pPb systems than in the PbPb system. For pPb collisions, $\langle \mathrm{KE_T} \rangle$ in the Pb-going direction for $\mathrm{K_S^0}$ ($\Lambda + \overline{\Lambda}$) is 6% (12%) larger than in the p-going direction for events with the highest particle multiplicities.

Acknowledgments

References

[1] E. Andersen et al., "Enhancement of central Λ, Ξ and Ω yields in Pb-Pb collisions at 158 A GeV/*c*", *Phys. Lett. B* **433** (1998) 209, `doi:10.1016/S0370-2693(98)00689-3`.

[2] STAR Collaboration, "Experimental and theoretical challenges in the search for the quark gluon plasma: The STAR Collaboration's critical assessment of the evidence from RHIC collisions", *Nucl. Phys. A* **757** (2005) 102, `doi:10.1016/j.nuclphysa.2005.03.085, arXiv:nucl-ex/0501009`.

[3] J. Rafelski and B. Muller, "Strangeness Production in the Quark-Gluon Plasma", *Phys. Rev. Lett.* **48** (1982) 1066, `doi:10.1103/PhysRevLett.48.1066`.

[4] STAR Collaboration, "Enhanced strange baryon production in Au + Au collisions compared to p + p at s(NN)**(1/2) = 200-GeV", *Phys. Rev. C* **77** (2008) 044908, `doi:10.1103/PhysRevC.77.044908, arXiv:0705.2511`.

[5] WA97 Collaboration, "Strangeness enhancement at mid-rapidity in Pb Pb collisions at 158-A-GeV/c", *Phys. Lett. B* **449** (1999) 401, `doi:10.1016/S0370-2693(99)00140-9`.

[6] STAR Collaboration, "Multistrange baryon production in Au-Au collisions at S(NN)**1/2 = 130 GeV", *Phys. Rev. Lett.* **92** (2004) 182301, `doi:10.1103/PhysRevLett.92.182301, arXiv:nucl-ex/0307024`.

[7] PHENIX Collaboration, "Formation of dense partonic matter in relativistic nucleus-nucleus collisions at RHIC: Experimental evaluation by the PHENIX Collaboration", *Nucl. Phys. A* **757** (2005) 184, `doi:10.1016/j.nuclphysa.2005.03.086, arXiv:nucl-ex/0410003`.

[8] CMS Collaboration, "Observation of long-range near-side angular correlations in proton-proton collisions at the LHC", *JHEP* **09** (2010) 091, `doi:10.1007/JHEP09(2010)091, arXiv:1009.4122`.

[9] CMS Collaboration, "Observation of long-range, near-side angular correlations in pPb collisions at the LHC", *Phys. Lett. B* **718** (2013) 795, `doi:10.1016/j.physletb.2012.11.025, arXiv:1210.5482`.

[10] ATLAS Collaboration, "Observation of associated near-side and away-side long-range correlations in $\sqrt{s_{NN}} = 5.02$ TeV proton-lead collisions with the ATLAS detector", *Phys. Rev. Lett.* **110** (2013) 182302, `doi:10.1103/PhysRevLett.110.182302`, `arXiv:1212.5198`.

[11] ALICE Collaboration, "Long-range angular correlations on the near and away side in pPb collisions at $\sqrt{s_{NN}} = 5.02$ TeV", *Phys. Lett. B* **719** (2013) 29, `doi:10.1016/j.physletb.2013.01.012`, `arXiv:1212.2001`.

[12] K. Dusling, W. Li, and B. Schenke, "Novel collective phenomena in high-energy proton-proton and proton-nucleus collisions", *Int. J. Mod. Phys. E* **25** (2016), no. 01, 1630002, `doi:10.1142/S0218301316300022`, `arXiv:1509.07939`.

[13] P. Bożek, "Collective flow in *p*-Pb and *d*-Pb collisions at TeV energies", *Phys. Rev. C* **85** (2012) 014911, `doi:10.1103/PhysRevC.85.014911`, `arXiv:1112.0915`.

[14] P. Bożek and W. Broniowski, "Correlations from hydrodynamic flow in pPb collisions", *Phys. Lett. B* **718** (2013) 1557, `doi:10.1016/j.physletb.2012.12.051`, `arXiv:1211.0845`.

[15] A. Bzdak, B. Schenke, P. Tribedy, and R. Venugopalan, "Initial state geometry and the role of hydrodynamics in proton-proton, proton-nucleus and deuteron-nucleus collisions", *Phys. Rev. C* **87** (2013) 064906, `doi:10.1103/PhysRevC.87.064906`, `arXiv:1304.3403`.

[16] K. Werner, I. Karpenko, and T. Pierog, ""Ridge" in Proton-Proton Scattering at 7 TeV", *Phys. Rev. Lett.* **106** (2011) 122004, `doi:10.1103/PhysRevLett.106.122004`, `arXiv:1011.0375`.

[17] K. Dusling and R. Venugopalan, "Explanation of systematics of CMS p+Pb high multiplicity di-hadron data at $\sqrt{s_{NN}} = 5.02$ TeV", *Phys. Rev. D* **87** (2013) 054014, `doi:10.1103/PhysRevD.87.054014`, `arXiv:1211.3701`.

[18] K. Dusling and R. Venugopalan, "Evidence for BFKL and saturation dynamics from dihadron spectra at the LHC", *Phys. Rev. D* **87** (2013) 051502, `doi:10.1103/PhysRevD.87.051502`, `arXiv:1210.3890`.

[19] A. Dumitru, L. McLerran, and V. Skokov, "Azimuthal asymmetries and the emergence of "collectivity" from multi-particle correlations in high-energy pA collisions", *Phys. Lett. B* **743** (2015) 134, `doi:10.1016/j.physletb.2015.02.046`, `arXiv:1410.4844`.

[20] M. Gyulassy, P. Levai, I. Vitev, and T. S. Biro, "Non-Abelian bremsstrahlung and azimuthal asymmetries in high energy $p + A$ reactions", *Phys. Rev. D* **90** (2014) 054025, `doi:10.1103/PhysRevD.90.054025`, `arXiv:1405.7825`.

[21] W. Li, "Observation of a 'ridge' correlation structure in high multiplicity proton-proton collisions: A brief review", *Mod. Phys. Lett. A* **27** (2012) 1230018, `doi:10.1142/S0217732312300182`, `arXiv:1206.0148`.

[22] L. He et al., "Anisotropic parton escape is the dominant source of azimuthal anisotropy in transport models", *Phys. Lett. B* **753** (2016) 506, `doi:10.1016/j.physletb.2015.12.051`, `arXiv:1502.05572`.

[23] ALICE Collaboration, "Centrality dependence of π, K, p production in Pb-Pb collisions at $\sqrt{s_{NN}}$ = 2.76 TeV", *Phys. Rev. C* **88** (2013) 044910, `doi:10.1103/PhysRevC.88.044910`, `arXiv:1303.0737`.

[24] ALICE Collaboration, "Elliptic flow of identified hadrons in Pb-Pb collisions at $\sqrt{s_{NN}}$ = 2.76 TeV", *JHEP* **06** (2015) 190, `doi:10.1007/JHEP06(2015)190`, `arXiv:1405.4632`.

[25] H. Song, S. Bass, and U. W. Heinz, "Spectra and elliptic flow for identified hadrons in 2.76A TeV Pb+Pb collisions", *Phys. Rev. C* **89** (2014) 034919, `doi:10.1103/PhysRevC.89.034919`, `arXiv:1311.0157`.

[26] X. Zhu, F. Meng, H. Song, and Y.-X. Liu, "Hybrid model approach for strange and multistrange hadrons in 2.76A TeV Pb+Pb collisions", *Phys. Rev. C* **91** (2015), no. 3, 034904, `doi:10.1103/PhysRevC.91.034904`, `arXiv:1501.03286`.

[27] ALICE Collaboration, "Multiplicity dependence of pion, kaon, proton and lambda production in p-Pb collisions at $\sqrt{s_{NN}}$ = 5.02 TeV", *Phys. Lett. B* **728** (2014) 25, `doi:10.1016/j.physletb.2013.11.020`, `arXiv:1307.6796`.

[28] CMS Collaboration, "Study of the production of charged pions, kaons, and protons in pPb collisions at $\sqrt{s_{NN}}$ = 5.02 TeV", *Eur. Phys. J. C* **74** (2014) 2847, `doi:10.1140/epjc/s10052-014-2847-x`, `arXiv:1307.3442`.

[29] ALICE Collaboration, "Long-range angular correlations of π, K and p in p–Pb collisions at $\sqrt{s_{NN}}$ = 5.02 TeV", *Phys. Lett. B* **726** (2013) 164, `doi:10.1016/j.physletb.2013.08.024`, `arXiv:1307.3237`.

[30] CMS Collaboration, "Long-range two-particle correlations of strange hadrons with charged particles in pPb and PbPb collisions at LHC energies", *Phys. Lett. B* **742** (2015) 200, `doi:10.1016/j.physletb.2015.01.034`, `arXiv:1409.3392`.

[31] E. Shuryak and I. Zahed, "High-multiplicity pp and pA collisions: Hydrodynamics at its edge", *Phys. Rev. C* **88** (2013) 044915, `doi:10.1103/PhysRevC.88.044915`, `arXiv:1301.4470`.

[32] E. Schnedermann, J. Sollfrank, and U. Heinz, "Thermal phenomenology of hadrons from 200 A GeV S+S collisions", *Phys. Rev. C* **48** (1993) 2462, `doi:10.1103/PhysRevC.48.2462`, `arXiv:nucl-th/9307020`.

[33] UA1 Collaboration, "A study of the general characteristics of proton-antiproton collisions at $\sqrt{s}$ = 0.2 TeV to 0.9 TeV", *Nucl. Phys. B* **335** (1990) 261, `doi:10.1016/0550-3213(90)90493-W`.

[34] T. Alexopoulos et al., "Multiplicity dependence of the transverse momentum spectrum for centrally produced hadrons in antiproton-proton collisions at $\sqrt{s}$ = 1.8 Tev", *Phys. Rev. Lett.* **60** (1988) 1622, `doi:10.1103/PhysRevLett.60.1622`.

[35] STAR Collaboration, "Systematic measurements of identified particle spectra in pp, d + Au and Au + Au collisions from STAR", *Phys. Rev. C* **79** (2009) 034909, `doi:10.1103/PhysRevC.79.034909`, `arXiv:0808.2041`.

[36] A. Ortiz Velasquez et al., "Color Reconnection and Flowlike Patterns in pp Collisions", *Phys. Rev. Lett.* **111** (2013) 042001, `doi:10.1103/PhysRevLett.111.042001`, `arXiv:1303.6326`.

[37] P. Bożek, A. Bzdak, and V. Skokov, "The rapidity dependence of the average transverse momentum in p+Pb collisions at the LHC: the color glass condensate versus hydrodynamics", *Phys. Lett. B* **728** (2014) 662, `doi:10.1016/j.physletb.2013.12.034`, `arXiv:1309.7358`.

[38] CMS Collaboration, "Description and performance of track and primary-vertex reconstruction with the CMS tracker", *JINST* **9** (2014) P10009, `doi:10.1088/1748-0221/9/10/P10009`, `arXiv:1405.6569`.

[39] CMS Collaboration, "The CMS experiment at the CERN LHC", *JINST* **3** (2008) S08004, `doi:10.1088/1748-0221/3/08/S08004`.

[40] Geant4 Collaboration, "Geant4: A simulation toolkit", *Nucl. Instrum. and Methods A* **506** (2003) 250, `doi:10.1016/S0168-9002(03)01368-8`.

[41] CMS Collaboration, "Multiplicity and transverse momentum dependence of two- and four-particle correlations in pPb and PbPb collisions", *Phys. Lett. B* **724** (2013) 213, `doi:10.1016/j.physletb.2013.06.028`, `arXiv:1305.0609`.

[42] CMS Collaboration, "Azimuthal anisotropy of charged particles at high transverse momenta in PbPb collisions at $\sqrt{s_{NN}} = 2.76$ TeV", *Phys. Rev. Lett.* **109** (2012) 022301, `doi:10.1103/PhysRevLett.109.022301`, `arXiv:1204.1850`.

[43] CMS Trigger and Data Acquisition Group Collaboration, "The CMS high level trigger", *Eur. Phys. J. C* **46** (2006) 605, `doi:10.1140/epjc/s2006-02495-8`, `arXiv:hep-ex/0512077`.

[44] T. Pierog et al., "EPOS LHC: Test of collective hadronization with data measured at the CERN Large Hadron Collider", *Phys. Rev. C* **92** (2015) 034906, `doi:10.1103/PhysRevC.92.034906`.

[45] M. Gyulassy and X.-N. Wang, "HIJING 1.0: A Monte Carlo program for parton and particle production in high-energy hadronic and nuclear collisions", *Comput. Phys. Commun.* **83** (1994) 307, `doi:10.1016/0010-4655(94)90057-4`, `arXiv:nucl-th/9502021`.

[46] T. Sjöstrand, S. Mrenna, and P. Skands, "PYTHIA 6.4 physics and manual", *JHEP* **05** (2006) 026, `doi:10.1088/1126-6708/2006/05/026`, `arXiv:hep-ph/0603175`.

[47] T. Sjöstrand, S. Mrenna, and P. Skands, "A brief introduction to PYTHIA 8.1", *Comp. Phys. Comm.* **178** (2008) 852, `doi:10.1016/j.cpc.2008.01.036`, `arXiv:0710.3820`.

[48] CMS Collaboration, "Measurement of Tracking Efficiency", CMS Physics Analysis Summary CMS-PAS-TRK-10-002, 2010.

[49] CMS Collaboration, "Strange particle production in pp collisions at $\sqrt{s} = 0.9$ and 7 TeV", *JHEP* **05** (2011) 064, `doi:10.1007/JHEP05(2011)064`, `arXiv:1102.4282`.

[50] Particle Data Group, K. A. Olive et al., "Review of Particle Physics", *Chin. Phys. C* **38** (2014) 090001, `doi:10.1088/1674-1137/38/9/090001`.

[51] P. Bożek and I. Wyskiel-Piekarska, "Particle spectra in Pb-Pb collisions at $\sqrt{s_{NN}} = 2.76$ TeV", *Phys. Rev. C* **85** (2012) 064915, `doi:10.1103/PhysRevC.85.064915`, `arXiv:1203.6513`.

[52] I. A. Karpenko, Yu. M. Sinyukov, and K. Werner, "Uniform description of bulk observables in the hydrokinetic model of $A + A$ collisions at the BNL Relativistic Heavy Ion Collider and the CERN Large Hadron Collider", *Phys. Rev. C* **87** (2013) 024914, `doi:10.1103/PhysRevC.87.024914`, `arXiv:1204.5351`.

[53] R. J. Fries, V. Greco, and P. Sorensen, "Coalescence Models For Hadron Formation From Quark Gluon Plasma", *Ann. Rev. Nucl. Part. Sci.* **58** (2008) 177, `doi:10.1146/annurev.nucl.58.110707.171134`, `arXiv:0807.4939`.

[54] CMS Collaboration, "Study of the inclusive production of charged pions, kaons, and protons in pp collisions at $\sqrt{s} = 0.9, 2.76,$ and 7 TeV", *Eur. Phys. J. C* **72** (2012) 2164, `doi:10.1140/epjc/s10052-012-2164-1`, `arXiv:1207.4724`.

[55] ALICE Collaboration, "Production of K* (892)^0 and ϕ (1020) in p-Pb collisions at $\sqrt{s_{\mathrm{NN}}} =$ 5.02 TeV", *Eur. Phys. J. C* **76** (2016), no. 5, 245, `doi:10.1140/epjc/s10052-016-4088-7`, `arXiv:1601.07868`.

A The CMS Collaboration

Yerevan Physics Institute, Yerevan, Armenia
V. Khachatryan, A.M. Sirunyan, A. Tumasyan

Institut für Hochenergiephysik der OeAW, Wien, Austria
W. Adam, E. Asilar, T. Bergauer, J. Brandstetter, E. Brondolin, M. Dragicevic, J. Erö, M. Flechl, M. Friedl, R. Frühwirth[1], V.M. Ghete, C. Hartl, N. Hörmann, J. Hrubec, M. Jeitler[1], A. König, M. Krammer[1], I. Krätschmer, D. Liko, T. Matsushita, I. Mikulec, D. Rabady, N. Rad, B. Rahbaran, H. Rohringer, J. Schieck[1], J. Strauss, W. Treberer-Treberspurg, W. Waltenberger, C.-E. Wulz[1]

National Centre for Particle and High Energy Physics, Minsk, Belarus
V. Mossolov, N. Shumeiko, J. Suarez Gonzalez

Universiteit Antwerpen, Antwerpen, Belgium
S. Alderweireldt, T. Cornelis, E.A. De Wolf, X. Janssen, A. Knutsson, J. Lauwers, S. Luyckx, M. Van De Klundert, H. Van Haevermaet, P. Van Mechelen, N. Van Remortel, A. Van Spilbeeck

Vrije Universiteit Brussel, Brussel, Belgium
S. Abu Zeid, F. Blekman, J. D'Hondt, N. Daci, I. De Bruyn, K. Deroover, N. Heracleous, J. Keaveney, S. Lowette, S. Moortgat, L. Moreels, A. Olbrechts, Q. Python, D. Strom, S. Tavernier, W. Van Doninck, P. Van Mulders, I. Van Parijs

Université Libre de Bruxelles, Bruxelles, Belgium
H. Brun, C. Caillol, B. Clerbaux, G. De Lentdecker, G. Fasanella, L. Favart, R. Goldouzian, A. Grebenyuk, G. Karapostoli, T. Lenzi, A. Léonard, T. Maerschalk, A. Marinov, A. Randle-conde, T. Seva, C. Vander Velde, P. Vanlaer, R. Yonamine, F. Zenoni, F. Zhang[2]

Ghent University, Ghent, Belgium
L. Benucci, A. Cimmino, S. Crucy, D. Dobur, A. Fagot, G. Garcia, M. Gul, J. Mccartin, A.A. Ocampo Rios, D. Poyraz, D. Ryckbosch, S. Salva, R. Schöfbeck, M. Sigamani, M. Tytgat, W. Van Driessche, E. Yazgan, N. Zaganidis

Université Catholique de Louvain, Louvain-la-Neuve, Belgium
C. Beluffi[3], O. Bondu, S. Brochet, G. Bruno, A. Caudron, L. Ceard, S. De Visscher, C. Delaere, M. Delcourt, L. Forthomme, B. Francois, A. Giammanco, A. Jafari, P. Jez, M. Komm, V. Lemaitre, A. Magitteri, A. Mertens, M. Musich, C. Nuttens, K. Piotrzkowski, L. Quertenmont, M. Selvaggi, M. Vidal Marono, S. Wertz

Université de Mons, Mons, Belgium
N. Beliy, G.H. Hammad

Centro Brasileiro de Pesquisas Fisicas, Rio de Janeiro, Brazil
W.L. Aldá Júnior, F.L. Alves, G.A. Alves, L. Brito, M. Correa Martins Junior, M. Hamer, C. Hensel, A. Moraes, M.E. Pol, P. Rebello Teles

Universidade do Estado do Rio de Janeiro, Rio de Janeiro, Brazil
E. Belchior Batista Das Chagas, W. Carvalho, J. Chinellato[4], A. Custódio, E.M. Da Costa, D. De Jesus Damiao, C. De Oliveira Martins, S. Fonseca De Souza, L.M. Huertas Guativa, H. Malbouisson, D. Matos Figueiredo, C. Mora Herrera, L. Mundim, H. Nogima, W.L. Prado Da Silva, A. Santoro, A. Sznajder, E.J. Tonelli Manganote[4], A. Vilela Pereira

Universidade Estadual Paulista [a], Universidade Federal do ABC [b], São Paulo, Brazil
S. Ahuja[a], C.A. Bernardes[b], A. De Souza Santos[b], S. Dogra[a], T.R. Fernandez Perez Tomei[a],

E.M. Gregores[b], P.G. Mercadante[b], C.S. Moon[a,5], S.F. Novaes[a], Sandra S. Padula[a], D. Romero Abad[b], J.C. Ruiz Vargas

Institute for Nuclear Research and Nuclear Energy, Sofia, Bulgaria
A. Aleksandrov, R. Hadjiiska, P. Iaydjiev, M. Rodozov, S. Stoykova, G. Sultanov, M. Vutova

University of Sofia, Sofia, Bulgaria
A. Dimitrov, I. Glushkov, L. Litov, B. Pavlov, P. Petkov

Beihang University, Beijing, China
W. Fang[6]

Institute of High Energy Physics, Beijing, China
M. Ahmad, J.G. Bian, G.M. Chen, H.S. Chen, M. Chen, T. Cheng, R. Du, C.H. Jiang, D. Leggat, R. Plestina[7], F. Romeo, S.M. Shaheen, A. Spiezia, J. Tao, C. Wang, Z. Wang, H. Zhang

State Key Laboratory of Nuclear Physics and Technology, Peking University, Beijing, China
C. Asawatangtrakuldee, Y. Ban, Q. Li, S. Liu, Y. Mao, S.J. Qian, D. Wang, Z. Xu

Universidad de Los Andes, Bogota, Colombia
C. Avila, A. Cabrera, L.F. Chaparro Sierra, C. Florez, J.P. Gomez, B. Gomez Moreno, J.C. Sanabria

University of Split, Faculty of Electrical Engineering, Mechanical Engineering and Naval Architecture, Split, Croatia
N. Godinovic, D. Lelas, I. Puljak, P.M. Ribeiro Cipriano

University of Split, Faculty of Science, Split, Croatia
Z. Antunovic, M. Kovac

Institute Rudjer Boskovic, Zagreb, Croatia
V. Brigljevic, D. Ferencek, K. Kadija, J. Luetic, S. Micanovic, L. Sudic

University of Cyprus, Nicosia, Cyprus
A. Attikis, G. Mavromanolakis, J. Mousa, C. Nicolaou, F. Ptochos, P.A. Razis, H. Rykaczewski

Charles University, Prague, Czech Republic
M. Finger[8], M. Finger Jr.[8]

Universidad San Francisco de Quito, Quito, Ecuador
E. Carrera Jarrin

Academy of Scientific Research and Technology of the Arab Republic of Egypt, Egyptian Network of High Energy Physics, Cairo, Egypt
Y. Assran[9,10], T. Elkafrawy[11], A. Ellithi Kamel[12,12], A. Mahrous[13]

National Institute of Chemical Physics and Biophysics, Tallinn, Estonia
B. Calpas, M. Kadastik, M. Murumaa, L. Perrini, M. Raidal, A. Tiko, C. Veelken

Department of Physics, University of Helsinki, Helsinki, Finland
P. Eerola, J. Pekkanen, M. Voutilainen

Helsinki Institute of Physics, Helsinki, Finland
J. Härkönen, V. Karimäki, R. Kinnunen, T. Lampén, K. Lassila-Perini, S. Lehti, T. Lindén, P. Luukka, T. Peltola, J. Tuominiemi, E. Tuovinen, L. Wendland

Lappeenranta University of Technology, Lappeenranta, Finland
J. Talvitie, T. Tuuva

DSM/IRFU, CEA/Saclay, Gif-sur-Yvette, France
M. Besancon, F. Couderc, M. Dejardin, D. Denegri, B. Fabbro, J.L. Faure, C. Favaro, F. Ferri, S. Ganjour, A. Givernaud, P. Gras, G. Hamel de Monchenault, P. Jarry, E. Locci, M. Machet, J. Malcles, J. Rander, A. Rosowsky, M. Titov, A. Zghiche

Laboratoire Leprince-Ringuet, Ecole Polytechnique, IN2P3-CNRS, Palaiseau, France
A. Abdulsalam, I. Antropov, S. Baffioni, F. Beaudette, P. Busson, L. Cadamuro, E. Chapon, C. Charlot, O. Davignon, L. Dobrzynski, R. Granier de Cassagnac, M. Jo, S. Lisniak, P. Miné, I.N. Naranjo, M. Nguyen, C. Ochando, G. Ortona, P. Paganini, P. Pigard, S. Regnard, R. Salerno, Y. Sirois, T. Strebler, Y. Yilmaz, A. Zabi

Institut Pluridisciplinaire Hubert Curien, Université de Strasbourg, Université de Haute Alsace Mulhouse, CNRS/IN2P3, Strasbourg, France
J.-L. Agram[14], J. Andrea, A. Aubin, D. Bloch, J.-M. Brom, M. Buttignol, E.C. Chabert, N. Chanon, C. Collard, E. Conte[14], X. Coubez, J.-C. Fontaine[14], D. Gelé, U. Goerlach, C. Goetzmann, A.-C. Le Bihan, J.A. Merlin[15], K. Skovpen, P. Van Hove

Centre de Calcul de l'Institut National de Physique Nucleaire et de Physique des Particules, CNRS/IN2P3, Villeurbanne, France
S. Gadrat

Université de Lyon, Université Claude Bernard Lyon 1, CNRS-IN2P3, Institut de Physique Nucléaire de Lyon, Villeurbanne, France
S. Beauceron, C. Bernet, G. Boudoul, E. Bouvier, C.A. Carrillo Montoya, R. Chierici, D. Contardo, B. Courbon, P. Depasse, H. El Mamouni, J. Fan, J. Fay, S. Gascon, M. Gouzevitch, B. Ille, F. Lagarde, I.B. Laktineh, M. Lethuillier, L. Mirabito, A.L. Pequegnot, S. Perries, A. Popov[16], J.D. Ruiz Alvarez, D. Sabes, V. Sordini, M. Vander Donckt, P. Verdier, S. Viret

Georgian Technical University, Tbilisi, Georgia
T. Toriashvili[17]

Tbilisi State University, Tbilisi, Georgia
Z. Tsamalaidze[8]

RWTH Aachen University, I. Physikalisches Institut, Aachen, Germany
C. Autermann, S. Beranek, L. Feld, A. Heister, M.K. Kiesel, K. Klein, M. Lipinski, A. Ostapchuk, M. Preuten, F. Raupach, S. Schael, C. Schomakers, J.F. Schulte, J. Schulz, T. Verlage, H. Weber, V. Zhukov[16]

RWTH Aachen University, III. Physikalisches Institut A, Aachen, Germany
M. Ata, M. Brodski, E. Dietz-Laursonn, D. Duchardt, M. Endres, M. Erdmann, S. Erdweg, T. Esch, R. Fischer, A. Güth, T. Hebbeker, C. Heidemann, K. Hoepfner, S. Knutzen, M. Merschmeyer, A. Meyer, P. Millet, S. Mukherjee, M. Olschewski, K. Padeken, P. Papacz, T. Pook, M. Radziej, H. Reithler, M. Rieger, F. Scheuch, L. Sonnenschein, D. Teyssier, S. Thüer

RWTH Aachen University, III. Physikalisches Institut B, Aachen, Germany
V. Cherepanov, Y. Erdogan, G. Flügge, H. Geenen, M. Geisler, F. Hoehle, B. Kargoll, T. Kress, A. Künsken, J. Lingemann, A. Nehrkorn, A. Nowack, I.M. Nugent, C. Pistone, O. Pooth, A. Stahl[15]

Deutsches Elektronen-Synchrotron, Hamburg, Germany
M. Aldaya Martin, I. Asin, K. Beernaert, O. Behnke, U. Behrens, K. Borras[18], A. Campbell, P. Connor, C. Contreras-Campana, F. Costanza, C. Diez Pardos, G. Dolinska, S. Dooling, G. Eckerlin, D. Eckstein, T. Eichhorn, E. Gallo[19], J. Garay Garcia, A. Geiser, A. Gizhko,

J.M. Grados Luyando, P. Gunnellini, A. Harb, J. Hauk, M. Hempel[20], H. Jung, A. Kalogeropoulos, O. Karacheban[20], M. Kasemann, J. Kieseler, C. Kleinwort, I. Korol, W. Lange, A. Lelek, J. Leonard, K. Lipka, A. Lobanov, W. Lohmann[20], R. Mankel, I.-A. Melzer-Pellmann, A.B. Meyer, G. Mittag, J. Mnich, A. Mussgiller, E. Ntomari, D. Pitzl, R. Placakyte, A. Raspereza, B. Roland, M.Ö. Sahin, P. Saxena, T. Schoerner-Sadenius, C. Seitz, S. Spannagel, N. Stefaniuk, K.D. Trippkewitz, G.P. Van Onsem, R. Walsh, C. Wissing

University of Hamburg, Hamburg, Germany
V. Blobel, M. Centis Vignali, A.R. Draeger, T. Dreyer, J. Erfle, E. Garutti, K. Goebel, D. Gonzalez, M. Görner, J. Haller, M. Hoffmann, R.S. Höing, A. Junkes, R. Klanner, R. Kogler, N. Kovalchuk, T. Lapsien, T. Lenz, I. Marchesini, D. Marconi, M. Meyer, M. Niedziela, D. Nowatschin, J. Ott, F. Pantaleo[15], T. Peiffer, A. Perieanu, N. Pietsch, J. Poehlsen, C. Sander, C. Scharf, P. Schleper, E. Schlieckau, A. Schmidt, S. Schumann, J. Schwandt, H. Stadie, G. Steinbrück, F.M. Stober, H. Tholen, D. Troendle, E. Usai, L. Vanelderen, A. Vanhoefer, B. Vormwald

Institut für Experimentelle Kernphysik, Karlsruhe, Germany
C. Barth, C. Baus, J. Berger, C. Böser, E. Butz, T. Chwalek, F. Colombo, W. De Boer, A. Descroix, A. Dierlamm, S. Fink, F. Frensch, R. Friese, M. Giffels, A. Gilbert, D. Haitz, F. Hartmann[15], S.M. Heindl, U. Husemann, I. Katkov[16], A. Kornmayer[15], P. Lobelle Pardo, B. Maier, H. Mildner, M.U. Mozer, T. Müller, Th. Müller, M. Plagge, G. Quast, K. Rabbertz, S. Röcker, F. Roscher, M. Schröder, G. Sieber, H.J. Simonis, R. Ulrich, J. Wagner-Kuhr, S. Wayand, M. Weber, T. Weiler, S. Williamson, C. Wöhrmann, R. Wolf

Institute of Nuclear and Particle Physics (INPP), NCSR Demokritos, Aghia Paraskevi, Greece
G. Anagnostou, G. Daskalakis, T. Geralis, V.A. Giakoumopoulou, A. Kyriakis, D. Loukas, A. Psallidas, I. Topsis-Giotis

National and Kapodistrian University of Athens, Athens, Greece
A. Agapitos, S. Kesisoglou, A. Panagiotou, N. Saoulidou, E. Tziaferi

University of Ioánnina, Ioánnina, Greece
I. Evangelou, G. Flouris, C. Foudas, P. Kokkas, N. Loukas, N. Manthos, I. Papadopoulos, E. Paradas, J. Strologas

MTA-ELTE Lendület CMS Particle and Nuclear Physics Group, Eötvös Loránd University
N. Filipovic

Wigner Research Centre for Physics, Budapest, Hungary
G. Bencze, C. Hajdu, P. Hidas, D. Horvath[21], F. Sikler, V. Veszpremi, G. Vesztergombi[22], A.J. Zsigmond

Institute of Nuclear Research ATOMKI, Debrecen, Hungary
N. Beni, S. Czellar, J. Karancsi[23], J. Molnar, Z. Szillasi

University of Debrecen, Debrecen, Hungary
M. Bartók[22], A. Makovec, P. Raics, Z.L. Trocsanyi, B. Ujvari

National Institute of Science Education and Research, Bhubaneswar, India
S. Choudhury[24], P. Mal, K. Mandal, A. Nayak, D.K. Sahoo, N. Sahoo, S.K. Swain

Panjab University, Chandigarh, India
S. Bansal, S.B. Beri, V. Bhatnagar, R. Chawla, R. Gupta, U.Bhawandeep, A.K. Kalsi, A. Kaur, M. Kaur, R. Kumar, A. Mehta, M. Mittal, J.B. Singh, G. Walia

University of Delhi, Delhi, India
Ashok Kumar, A. Bhardwaj, B.C. Choudhary, R.B. Garg, S. Keshri, A. Kumar, S. Malhotra, M. Naimuddin, N. Nishu, K. Ranjan, R. Sharma, V. Sharma

Saha Institute of Nuclear Physics, Kolkata, India
R. Bhattacharya, S. Bhattacharya, K. Chatterjee, S. Dey, S. Dutta, S. Ghosh, N. Majumdar, A. Modak, K. Mondal, S. Mukhopadhyay, S. Nandan, A. Purohit, A. Roy, D. Roy, S. Roy Chowdhury, S. Sarkar, M. Sharan

Bhabha Atomic Research Centre, Mumbai, India
R. Chudasama, D. Dutta, V. Jha, V. Kumar, A.K. Mohanty[15], L.M. Pant, P. Shukla, A. Topkar

Tata Institute of Fundamental Research, Mumbai, India
T. Aziz, S. Banerjee, S. Bhowmik[25], R.M. Chatterjee, R.K. Dewanjee, S. Dugad, S. Ganguly, S. Ghosh, M. Guchait, A. Gurtu[26], Sa. Jain, G. Kole, S. Kumar, B. Mahakud, M. Maity[25], G. Majumder, K. Mazumdar, S. Mitra, G.B. Mohanty, B. Parida, T. Sarkar[25], N. Sur, B. Sutar, N. Wickramage[27]

Indian Institute of Science Education and Research (IISER), Pune, India
S. Chauhan, S. Dube, A. Kapoor, K. Kothekar, A. Rane, S. Sharma

Institute for Research in Fundamental Sciences (IPM), Tehran, Iran
H. Bakhshiansohi, H. Behnamian, S.M. Etesami[28], A. Fahim[29], M. Khakzad, M. Mohammadi Najafabadi, M. Naseri, S. Paktinat Mehdiabadi, F. Rezaei Hosseinabadi, B. Safarzadeh[30], M. Zeinali

University College Dublin, Dublin, Ireland
M. Felcini, M. Grunewald

INFN Sezione di Bari [a], Università di Bari [b], Politecnico di Bari [c], Bari, Italy
M. Abbrescia[a,b], C. Calabria[a,b], C. Caputo[a,b], A. Colaleo[a], D. Creanza[a,c], L. Cristella[a,b], N. De Filippis[a,c], M. De Palma[a,b], L. Fiore[a], G. Iaselli[a,c], G. Maggi[a,c], M. Maggi[a], G. Miniello[a,b], S. My[a,b], S. Nuzzo[a,b], A. Pompili[a,b], G. Pugliese[a,c], R. Radogna[a,b], A. Ranieri[a], G. Selvaggi[a,b], L. Silvestris[a,15], R. Venditti[a,b]

INFN Sezione di Bologna [a], Università di Bologna [b], Bologna, Italy
G. Abbiendi[a], C. Battilana, D. Bonacorsi[a,b], S. Braibant-Giacomelli[a,b], L. Brigliadori[a,b], R. Campanini[a,b], P. Capiluppi[a,b], A. Castro[a,b], F.R. Cavallo[a], S.S. Chhibra[a,b], G. Codispoti[a,b], M. Cuffiani[a,b], G.M. Dallavalle[a], F. Fabbri[a], A. Fanfani[a,b], D. Fasanella[a,b], P. Giacomelli[a], C. Grandi[a], L. Guiducci[a,b], S. Marcellini[a], G. Masetti[a], A. Montanari[a], F.L. Navarria[a,b], A. Perrotta[a], A.M. Rossi[a,b], T. Rovelli[a,b], G.P. Siroli[a,b], N. Tosi[a,b,15]

INFN Sezione di Catania [a], Università di Catania [b], Catania, Italy
G. Cappello[b], M. Chiorboli[a,b], S. Costa[a,b], A. Di Mattia[a], F. Giordano[a,b], R. Potenza[a,b], A. Tricomi[a,b], C. Tuve[a,b]

INFN Sezione di Firenze [a], Università di Firenze [b], Firenze, Italy
G. Barbagli[a], V. Ciulli[a,b], C. Civinini[a], R. D'Alessandro[a,b], E. Focardi[a,b], V. Gori[a,b], P. Lenzi[a,b], M. Meschini[a], S. Paoletti[a], G. Sguazzoni[a], L. Viliani[a,b,15]

INFN Laboratori Nazionali di Frascati, Frascati, Italy
L. Benussi, S. Bianco, F. Fabbri, D. Piccolo, F. Primavera[15]

INFN Sezione di Genova [a], Università di Genova [b], Genova, Italy
V. Calvelli[a,b], F. Ferro[a], M. Lo Vetere[a,b], M.R. Monge[a,b], E. Robutti[a], S. Tosi[a,b]

INFN Sezione di Milano-Bicocca [a], **Università di Milano-Bicocca** [b], **Milano, Italy**

L. Brianza, M.E. Dinardo[a,b], S. Fiorendi[a,b], S. Gennai[a], A. Ghezzi[a,b], P. Govoni[a,b], S. Malvezzi[a], R.A. Manzoni[a,b,15], B. Marzocchi[a,b], D. Menasce[a], L. Moroni[a], M. Paganoni[a,b], D. Pedrini[a], S. Pigazzini, S. Ragazzi[a,b], N. Redaelli[a], T. Tabarelli de Fatis[a,b]

INFN Sezione di Napoli [a], **Università di Napoli 'Federico II'** [b], **Napoli, Italy, Università della Basilicata** [c], **Potenza, Italy, Università G. Marconi** [d], **Roma, Italy**

S. Buontempo[a], N. Cavallo[a,c], S. Di Guida[a,d,15], M. Esposito[a,b], F. Fabozzi[a,c], A.O.M. Iorio[a,b], G. Lanza[a], L. Lista[a], S. Meola[a,d,15], M. Merola[a], P. Paolucci[a,15], C. Sciacca[a,b], F. Thyssen

INFN Sezione di Padova [a], **Università di Padova** [b], **Padova, Italy, Università di Trento** [c], **Trento, Italy**

P. Azzi[a,15], N. Bacchetta[a], M. Bellato[a], L. Benato[a,b], A. Boletti[a,b], M. Dall'Osso[a,b], P. De Castro Manzano[a], T. Dorigo[a], F. Fanzago[a], F. Gonella[a], A. Gozzelino[a], S. Lacaprara[a], M. Margoni[a,b], G. Maron[a,31], A.T. Meneguzzo[a,b], F. Montecassiano[a], M. Passaseo[a], J. Pazzini[a,b,15], M. Pegoraro[a], N. Pozzobon[a,b], P. Ronchese[a,b], M. Sgaravatto[a], F. Simonetto[a,b], E. Torassa[a], M. Tosi[a,b], S. Vanini[a,b], S. Ventura[a], M. Zanetti, P. Zotto[a,b], A. Zucchetta[a,b]

INFN Sezione di Pavia [a], **Università di Pavia** [b], **Pavia, Italy**

A. Braghieri[a], A. Magnani[a,b], P. Montagna[a,b], S.P. Ratti[a,b], V. Re[a], C. Riccardi[a,b], P. Salvini[a], I. Vai[a,b], P. Vitulo[a,b]

INFN Sezione di Perugia [a], **Università di Perugia** [b], **Perugia, Italy**

L. Alunni Solestizi[a,b], G.M. Bilei[a], D. Ciangottini[a,b], L. Fanò[a,b], P. Lariccia[a,b], R. Leonardi[a,b], G. Mantovani[a,b], M. Menichelli[a], A. Saha[a], A. Santocchia[a,b]

INFN Sezione di Pisa [a], **Università di Pisa** [b], **Scuola Normale Superiore di Pisa** [c], **Pisa, Italy**

K. Androsov[a,32], P. Azzurri[a,15], G. Bagliesi[a], J. Bernardini[a], T. Boccali[a], R. Castaldi[a], M.A. Ciocci[a,32], R. Dell'Orso[a], S. Donato[a,c], G. Fedi, A. Giassi[a], M.T. Grippo[a,32], F. Ligabue[a,c], T. Lomtadze[a], L. Martini[a,b], A. Messineo[a,b], F. Palla[a], A. Rizzi[a,b], A. Savoy-Navarro[a,33], P. Spagnolo[a], R. Tenchini[a], G. Tonelli[a,b], A. Venturi[a], P.G. Verdini[a]

INFN Sezione di Roma [a], **Università di Roma** [b], **Roma, Italy**

L. Barone[a,b], F. Cavallari[a], G. D'imperio[a,b,15], D. Del Re[a,b,15], M. Diemoz[a], S. Gelli[a,b], C. Jorda[a], E. Longo[a,b], F. Margaroli[a,b], P. Meridiani[a], G. Organtini[a,b], R. Paramatti[a], F. Preiato[a,b], S. Rahatlou[a,b], C. Rovelli[a], F. Santanastasio[a,b]

INFN Sezione di Torino [a], **Università di Torino** [b], **Torino, Italy, Università del Piemonte Orientale** [c], **Novara, Italy**

N. Amapane[a,b], R. Arcidiacono[a,c,15], S. Argiro[a,b], M. Arneodo[a,c], N. Bartosik[a], R. Bellan[a,b], C. Biino[a], N. Cartiglia[a], M. Costa[a,b], R. Covarelli[a,b], A. Degano[a,b], N. Demaria[a], L. Finco[a,b], B. Kiani[a,b], C. Mariotti[a], S. Maselli[a], E. Migliore[a,b], V. Monaco[a,b], E. Monteil[a,b], M.M. Obertino[a,b], L. Pacher[a,b], N. Pastrone[a], M. Pelliccioni[a], G.L. Pinna Angioni[a,b], F. Ravera[a,b], A. Romero[a,b], M. Ruspa[a,c], R. Sacchi[a,b], V. Sola[a], A. Solano[a,b], A. Staiano[a], P. Traczyk[a,b]

INFN Sezione di Trieste [a], **Università di Trieste** [b], **Trieste, Italy**

S. Belforte[a], V. Candelise[a,b], M. Casarsa[a], F. Cossutti[a], G. Della Ricca[a,b], C. La Licata[a,b], A. Schizzi[a,b], A. Zanetti[a]

Kangwon National University, Chunchon, Korea

S.K. Nam

Kyungpook National University, Daegu, Korea

D.H. Kim, G.N. Kim, M.S. Kim, D.J. Kong, S. Lee, S.W. Lee, Y.D. Oh, A. Sakharov, D.C. Son, Y.C. Yang

Chonbuk National University, Jeonju, Korea
J.A. Brochero Cifuentes, H. Kim, T.J. Kim[34]

Chonnam National University, Institute for Universe and Elementary Particles, Kwangju, Korea
S. Song

Korea University, Seoul, Korea
S. Cho, S. Choi, Y. Go, D. Gyun, B. Hong, Y. Jo, Y. Kim, B. Lee, K. Lee, K.S. Lee, S. Lee, J. Lim, S.K. Park, Y. Roh

Seoul National University, Seoul, Korea
H.D. Yoo

University of Seoul, Seoul, Korea
M. Choi, H. Kim, H. Kim, J.H. Kim, J.S.H. Lee, I.C. Park, G. Ryu, M.S. Ryu

Sungkyunkwan University, Suwon, Korea
Y. Choi, J. Goh, D. Kim, E. Kwon, J. Lee, I. Yu

Vilnius University, Vilnius, Lithuania
V. Dudenas, A. Juodagalvis, J. Vaitkus

National Centre for Particle Physics, Universiti Malaya, Kuala Lumpur, Malaysia
I. Ahmed, Z.A. Ibrahim, J.R. Komaragiri, M.A.B. Md Ali[35], F. Mohamad Idris[36], W.A.T. Wan Abdullah, M.N. Yusli, Z. Zolkapli

Centro de Investigacion y de Estudios Avanzados del IPN, Mexico City, Mexico
E. Casimiro Linares, H. Castilla-Valdez, E. De La Cruz-Burelo, I. Heredia-De La Cruz[37], A. Hernandez-Almada, R. Lopez-Fernandez, J. Mejia Guisao, A. Sanchez-Hernandez

Universidad Iberoamericana, Mexico City, Mexico
S. Carrillo Moreno, F. Vazquez Valencia

Benemerita Universidad Autonoma de Puebla, Puebla, Mexico
I. Pedraza, H.A. Salazar Ibarguen, C. Uribe Estrada

Universidad Autónoma de San Luis Potosí, San Luis Potosí, Mexico
A. Morelos Pineda

University of Auckland, Auckland, New Zealand
D. Krofcheck

University of Canterbury, Christchurch, New Zealand
P.H. Butler

National Centre for Physics, Quaid-I-Azam University, Islamabad, Pakistan
A. Ahmad, M. Ahmad, Q. Hassan, H.R. Hoorani, W.A. Khan, T. Khurshid, M. Shoaib, M. Waqas

National Centre for Nuclear Research, Swierk, Poland
H. Bialkowska, M. Bluj, B. Boimska, T. Frueboes, M. Górski, M. Kazana, K. Nawrocki, K. Romanowska-Rybinska, M. Szleper, P. Zalewski

Institute of Experimental Physics, Faculty of Physics, University of Warsaw, Warsaw, Poland
G. Brona, K. Bunkowski, A. Byszuk[38], K. Doroba, A. Kalinowski, M. Konecki, J. Krolikowski, M. Misiura, M. Olszewski, M. Walczak

Laboratório de Instrumentação e Física Experimental de Partículas, Lisboa, Portugal
P. Bargassa, C. Beirão Da Cruz E Silva, A. Di Francesco, P. Faccioli, P.G. Ferreira Parracho, M. Gallinaro, J. Hollar, N. Leonardo, L. Lloret Iglesias, M.V. Nemallapudi, F. Nguyen, J. Rodrigues Antunes, J. Seixas, O. Toldaiev, D. Vadruccio, J. Varela, P. Vischia

Joint Institute for Nuclear Research, Dubna, Russia
S. Afanasiev, P. Bunin, M. Gavrilenko, I. Golutvin, I. Gorbunov, A. Kamenev, V. Karjavin, A. Lanev, A. Malakhov, V. Matveev[39,40], P. Moisenz, V. Palichik, V. Perelygin, S. Shmatov, S. Shulha, N. Skatchkov, V. Smirnov, N. Voytishin, A. Zarubin

Petersburg Nuclear Physics Institute, Gatchina (St. Petersburg), Russia
V. Golovtsov, Y. Ivanov, V. Kim[41], E. Kuznetsova[42], P. Levchenko, V. Murzin, V. Oreshkin, I. Smirnov, V. Sulimov, L. Uvarov, S. Vavilov, A. Vorobyev

Institute for Nuclear Research, Moscow, Russia
Yu. Andreev, A. Dermenev, S. Gninenko, N. Golubev, A. Karneyeu, M. Kirsanov, N. Krasnikov, A. Pashenkov, D. Tlisov, A. Toropin

Institute for Theoretical and Experimental Physics, Moscow, Russia
V. Epshteyn, V. Gavrilov, N. Lychkovskaya, V. Popov, I. Pozdnyakov, G. Safronov, A. Spiridonov, M. Toms, E. Vlasov, A. Zhokin

National Research Nuclear University 'Moscow Engineering Physics Institute' (MEPhI), Moscow, Russia
M. Chadeeva, O. Markin, E. Popova, V. Rusinov, E. Tarkovskii

P.N. Lebedev Physical Institute, Moscow, Russia
V. Andreev, M. Azarkin[40], I. Dremin[40], M. Kirakosyan, A. Leonidov[40], G. Mesyats, S.V. Rusakov

Skobeltsyn Institute of Nuclear Physics, Lomonosov Moscow State University, Moscow, Russia
A. Baskakov, A. Belyaev, E. Boos, A. Ershov, A. Gribushin, V. Klyukhin, O. Kodolova, V. Korotkikh, I. Lokhtin, I. Miagkov, S. Obraztsov, S. Petrushanko, V. Savrin, A. Snigirev, I. Vardanyan

State Research Center of Russian Federation, Institute for High Energy Physics, Protvino, Russia
I. Azhgirey, I. Bayshev, S. Bitioukov, V. Kachanov, A. Kalinin, D. Konstantinov, V. Krychkine, V. Petrov, R. Ryutin, A. Sobol, L. Tourtchanovitch, S. Troshin, N. Tyurin, A. Uzunian, A. Volkov

University of Belgrade, Faculty of Physics and Vinca Institute of Nuclear Sciences, Belgrade, Serbia
P. Adzic[43], P. Cirkovic, D. Devetak, J. Milosevic, V. Rekovic

Centro de Investigaciones Energéticas Medioambientales y Tecnológicas (CIEMAT), Madrid, Spain
J. Alcaraz Maestre, E. Calvo, M. Cerrada, M. Chamizo Llatas, N. Colino, B. De La Cruz, A. Delgado Peris, A. Escalante Del Valle, C. Fernandez Bedoya, J.P. Fernández Ramos, J. Flix, M.C. Fouz, P. Garcia-Abia, O. Gonzalez Lopez, S. Goy Lopez, J.M. Hernandez, M.I. Josa, E. Navarro De Martino, A. Pérez-Calero Yzquierdo, J. Puerta Pelayo, A. Quintario Olmeda, I. Redondo, L. Romero, M.S. Soares

Universidad Autónoma de Madrid, Madrid, Spain
J.F. de Trocóniz, M. Missiroli, D. Moran

Universidad de Oviedo, Oviedo, Spain
J. Cuevas, J. Fernandez Menendez, S. Folgueras, I. Gonzalez Caballero, E. Palencia Cortezon, J.M. Vizan Garcia

Instituto de Física de Cantabria (IFCA), CSIC-Universidad de Cantabria, Santander, Spain
I.J. Cabrillo, A. Calderon, J.R. Castiñeiras De Saa, E. Curras, M. Fernandez, J. Garcia-Ferrero, G. Gomez, A. Lopez Virto, J. Marco, R. Marco, C. Martinez Rivero, F. Matorras, J. Piedra Gomez, T. Rodrigo, A.Y. Rodríguez-Marrero, A. Ruiz-Jimeno, L. Scodellaro, N. Trevisani, I. Vila, R. Vilar Cortabitarte

CERN, European Organization for Nuclear Research, Geneva, Switzerland
D. Abbaneo, E. Auffray, G. Auzinger, M. Bachtis, P. Baillon, A.H. Ball, D. Barney, A. Benaglia, L. Benhabib, G.M. Berruti, P. Bloch, A. Bocci, A. Bonato, C. Botta, H. Breuker, T. Camporesi, R. Castello, M. Cepeda, G. Cerminara, M. D'Alfonso, D. d'Enterria, A. Dabrowski, V. Daponte, A. David, M. De Gruttola, F. De Guio, A. De Roeck, E. Di Marco[44], M. Dobson, M. Dordevic, B. Dorney, T. du Pree, D. Duggan, M. Dünser, N. Dupont, A. Elliott-Peisert, S. Fartoukh, G. Franzoni, J. Fulcher, W. Funk, D. Gigi, K. Gill, M. Girone, F. Glege, R. Guida, S. Gundacker, M. Guthoff, J. Hammer, P. Harris, J. Hegeman, V. Innocente, P. Janot, H. Kirschenmann, V. Knünz, M.J. Kortelainen, K. Kousouris, P. Lecoq, C. Lourenço, M.T. Lucchini, N. Magini, L. Malgeri, M. Mannelli, A. Martelli, L. Masetti, F. Meijers, S. Mersi, E. Meschi, F. Moortgat, S. Morovic, M. Mulders, H. Neugebauer, S. Orfanelli[45], L. Orsini, L. Pape, E. Perez, M. Peruzzi, A. Petrilli, G. Petrucciani, A. Pfeiffer, M. Pierini, D. Piparo, A. Racz, T. Reis, G. Rolandi[46], M. Rovere, M. Ruan, H. Sakulin, J.B. Sauvan, C. Schäfer, C. Schwick, M. Seidel, A. Sharma, P. Silva, M. Simon, P. Sphicas[47], J. Steggemann, M. Stoye, Y. Takahashi, D. Treille, A. Triossi, A. Tsirou, V. Veckalns[48], G.I. Veres[22], N. Wardle, H.K. Wöhri, A. Zagozdzinska[38], W.D. Zeuner

Paul Scherrer Institut, Villigen, Switzerland
W. Bertl, K. Deiters, W. Erdmann, R. Horisberger, Q. Ingram, H.C. Kaestli, D. Kotlinski, U. Langenegger, T. Rohe

Institute for Particle Physics, ETH Zurich, Zurich, Switzerland
F. Bachmair, L. Bäni, L. Bianchini, B. Casal, G. Dissertori, M. Dittmar, M. Donegà, P. Eller, C. Grab, C. Heidegger, D. Hits, J. Hoss, G. Kasieczka, P. Lecomte[†], W. Lustermann, B. Mangano, M. Marionneau, P. Martinez Ruiz del Arbol, M. Masciovecchio, M.T. Meinhard, D. Meister, F. Micheli, P. Musella, F. Nessi-Tedaldi, F. Pandolfi, J. Pata, F. Pauss, G. Perrin, L. Perrozzi, M. Quittnat, M. Rossini, M. Schönenberger, A. Starodumov[49], M. Takahashi, V.R. Tavolaro, K. Theofilatos, R. Wallny

Universität Zürich, Zurich, Switzerland
T.K. Aarrestad, C. Amsler[50], L. Caminada, M.F. Canelli, V. Chiochia, A. De Cosa, C. Galloni, A. Hinzmann, T. Hreus, B. Kilminster, C. Lange, J. Ngadiuba, D. Pinna, G. Rauco, P. Robmann, D. Salerno, Y. Yang

National Central University, Chung-Li, Taiwan
K.H. Chen, T.H. Doan, Sh. Jain, R. Khurana, M. Konyushikhin, C.M. Kuo, W. Lin, Y.J. Lu, A. Pozdnyakov, S.S. Yu

National Taiwan University (NTU), Taipei, Taiwan
Arun Kumar, P. Chang, Y.H. Chang, Y.W. Chang, Y. Chao, K.F. Chen, P.H. Chen, C. Dietz, F. Fiori, W.-S. Hou, Y. Hsiung, Y.F. Liu, R.-S. Lu, M. Miñano Moya, J.f. Tsai, Y.M. Tzeng

Chulalongkorn University, Faculty of Science, Department of Physics, Bangkok, Thailand
B. Asavapibhop, K. Kovitanggoon, G. Singh, N. Srimanobhas, N. Suwonjandee

Cukurova University, Adana, Turkey
A. Adiguzel, S. Cerci[51], S. Damarseckin, Z.S. Demiroglu, C. Dozen, I. Dumanoglu, S. Girgis,
G. Gokbulut, Y. Guler, E. Gurpinar, I. Hos, E.E. Kangal[52], A. Kayis Topaksu, G. Onengut[53],
K. Ozdemir[54], A. Polatoz, B. Tali[51], H. Topakli[55], C. Zorbilmez

Middle East Technical University, Physics Department, Ankara, Turkey
B. Bilin, S. Bilmis, B. Isildak[56], G. Karapinar[57], M. Yalvac, M. Zeyrek

Bogazici University, Istanbul, Turkey
E. Gülmez, M. Kaya[58], O. Kaya[59], E.A. Yetkin[60], T. Yetkin[61]

Istanbul Technical University, Istanbul, Turkey
A. Cakir, K. Cankocak, S. Sen[62], F.I. Vardarlı

Institute for Scintillation Materials of National Academy of Science of Ukraine, Kharkov, Ukraine
B. Grynyov

National Scientific Center, Kharkov Institute of Physics and Technology, Kharkov, Ukraine
L. Levchuk, P. Sorokin

University of Bristol, Bristol, United Kingdom
R. Aggleton, F. Ball, L. Beck, J.J. Brooke, D. Burns, E. Clement, D. Cussans, H. Flacher,
J. Goldstein, M. Grimes, G.P. Heath, H.F. Heath, J. Jacob, L. Kreczko, C. Lucas, Z. Meng,
D.M. Newbold[63], S. Paramesvaran, A. Poll, T. Sakuma, S. Seif El Nasr-storey, S. Senkin,
D. Smith, V.J. Smith

Rutherford Appleton Laboratory, Didcot, United Kingdom
A. Belyaev[64], C. Brew, R.M. Brown, L. Calligaris, D. Cieri, D.J.A. Cockerill, J.A. Coughlan,
K. Harder, S. Harper, E. Olaiya, D. Petyt, C.H. Shepherd-Themistocleous, A. Thea, I.R. Tomalin,
T. Williams, S.D. Worm

Imperial College, London, United Kingdom
M. Baber, R. Bainbridge, O. Buchmuller, A. Bundock, D. Burton, S. Casasso, M. Citron,
D. Colling, L. Corpe, P. Dauncey, G. Davies, A. De Wit, M. Della Negra, P. Dunne, A. Elwood,
D. Futyan, Y. Haddad, G. Hall, G. Iles, R. Lane, R. Lucas[63], L. Lyons, A.-M. Magnan, S. Malik,
L. Mastrolorenzo, J. Nash, A. Nikitenko[49], J. Pela, B. Penning, M. Pesaresi, D.M. Raymond,
A. Richards, A. Rose, C. Seez, A. Tapper, K. Uchida, M. Vazquez Acosta[65], T. Virdee[15], S.C. Zenz

Brunel University, Uxbridge, United Kingdom
J.E. Cole, P.R. Hobson, A. Khan, P. Kyberd, D. Leslie, I.D. Reid, P. Symonds, L. Teodorescu,
M. Turner

Baylor University, Waco, USA
A. Borzou, K. Call, J. Dittmann, K. Hatakeyama, H. Liu, N. Pastika

The University of Alabama, Tuscaloosa, USA
O. Charaf, S.I. Cooper, C. Henderson, P. Rumerio

Boston University, Boston, USA
D. Arcaro, A. Avetisyan, T. Bose, D. Gastler, D. Rankin, C. Richardson, J. Rohlf, L. Sulak, D. Zou

Brown University, Providence, USA
J. Alimena, G. Benelli, E. Berry, D. Cutts, A. Ferapontov, A. Garabedian, J. Hakala, U. Heintz, O. Jesus, E. Laird, G. Landsberg, Z. Mao, M. Narain, S. Piperov, S. Sagir, R. Syarif

University of California, Davis, Davis, USA
R. Breedon, G. Breto, M. Calderon De La Barca Sanchez, S. Chauhan, M. Chertok, J. Conway, R. Conway, P.T. Cox, R. Erbacher, C. Flores, G. Funk, M. Gardner, W. Ko, R. Lander, C. Mclean, M. Mulhearn, D. Pellett, J. Pilot, F. Ricci-Tam, S. Shalhout, J. Smith, M. Squires, D. Stolp, M. Tripathi, S. Wilbur, R. Yohay

University of California, Los Angeles, USA
R. Cousins, P. Everaerts, A. Florent, J. Hauser, M. Ignatenko, D. Saltzberg, E. Takasugi, V. Valuev, M. Weber

University of California, Riverside, Riverside, USA
K. Burt, R. Clare, J. Ellison, J.W. Gary, G. Hanson, J. Heilman, P. Jandir, E. Kennedy, F. Lacroix, O.R. Long, M. Malberti, M. Olmedo Negrete, M.I. Paneva, A. Shrinivas, H. Wei, S. Wimpenny, B. R. Yates

University of California, San Diego, La Jolla, USA
J.G. Branson, G.B. Cerati, S. Cittolin, R.T. D'Agnolo, M. Derdzinski, R. Gerosa, A. Holzner, R. Kelley, D. Klein, J. Letts, I. Macneill, D. Olivito, S. Padhi, M. Pieri, M. Sani, V. Sharma, S. Simon, M. Tadel, A. Vartak, S. Wasserbaech[66], C. Welke, J. Wood, F. Würthwein, A. Yagil, G. Zevi Della Porta

University of California, Santa Barbara, Santa Barbara, USA
J. Bradmiller-Feld, C. Campagnari, A. Dishaw, V. Dutta, K. Flowers, M. Franco Sevilla, P. Geffert, C. George, F. Golf, L. Gouskos, J. Gran, J. Incandela, N. Mccoll, S.D. Mullin, J. Richman, D. Stuart, I. Suarez, C. West, J. Yoo

California Institute of Technology, Pasadena, USA
D. Anderson, A. Apresyan, J. Bendavid, A. Bornheim, J. Bunn, Y. Chen, J. Duarte, A. Mott, H.B. Newman, C. Pena, M. Spiropulu, J.R. Vlimant, S. Xie, R.Y. Zhu

Carnegie Mellon University, Pittsburgh, USA
M.B. Andrews, V. Azzolini, A. Calamba, B. Carlson, T. Ferguson, M. Paulini, J. Russ, M. Sun, H. Vogel, I. Vorobiev

University of Colorado Boulder, Boulder, USA
J.P. Cumalat, W.T. Ford, F. Jensen, A. Johnson, M. Krohn, T. Mulholland, K. Stenson, S.R. Wagner

Cornell University, Ithaca, USA
J. Alexander, A. Chatterjee, J. Chaves, J. Chu, S. Dittmer, N. Eggert, N. Mirman, G. Nicolas Kaufman, J.R. Patterson, A. Rinkevicius, A. Ryd, L. Skinnari, L. Soffi, W. Sun, S.M. Tan, W.D. Teo, J. Thom, J. Thompson, J. Tucker, Y. Weng, P. Wittich

Fermi National Accelerator Laboratory, Batavia, USA
S. Abdullin, M. Albrow, G. Apollinari, S. Banerjee, L.A.T. Bauerdick, A. Beretvas, J. Berryhill, P.C. Bhat, G. Bolla, K. Burkett, J.N. Butler, H.W.K. Cheung, F. Chlebana, S. Cihangir, M. Cremonesi, V.D. Elvira, I. Fisk, J. Freeman, E. Gottschalk, L. Gray, D. Green, S. Grünendahl, O. Gutsche, D. Hare, R.M. Harris, S. Hasegawa, J. Hirschauer, Z. Hu, B. Jayatilaka, S. Jindariani, M. Johnson, U. Joshi, B. Klima, B. Kreis, S. Lammel, J. Lewis, J. Linacre, D. Lincoln, R. Lipton, T. Liu, R. Lopes De Sá, J. Lykken, K. Maeshima, J.M. Marraffino, S. Maruyama, D. Mason,

P. McBride, P. Merkel, S. Mrenna, S. Nahn, C. Newman-Holmes[†], V. O'Dell, K. Pedro, O. Prokofyev, G. Rakness, E. Sexton-Kennedy, A. Soha, W.J. Spalding, L. Spiegel, S. Stoynev, N. Strobbe, L. Taylor, S. Tkaczyk, N.V. Tran, L. Uplegger, E.W. Vaandering, C. Vernieri, M. Verzocchi, R. Vidal, M. Wang, H.A. Weber, A. Whitbeck

University of Florida, Gainesville, USA
D. Acosta, P. Avery, P. Bortignon, D. Bourilkov, A. Brinkerhoff, A. Carnes, M. Carver, D. Curry, S. Das, R.D. Field, I.K. Furic, J. Konigsberg, A. Korytov, K. Kotov, P. Ma, K. Matchev, H. Mei, P. Milenovic[67], G. Mitselmakher, D. Rank, R. Rossin, L. Shchutska, D. Sperka, N. Terentyev, L. Thomas, J. Wang, S. Wang, J. Yelton

Florida International University, Miami, USA
S. Linn, P. Markowitz, G. Martinez, J.L. Rodriguez

Florida State University, Tallahassee, USA
A. Ackert, J.R. Adams, T. Adams, A. Askew, S. Bein, J. Bochenek, B. Diamond, J. Haas, S. Hagopian, V. Hagopian, K.F. Johnson, A. Khatiwada, H. Prosper, A. Santra, M. Weinberg

Florida Institute of Technology, Melbourne, USA
M.M. Baarmand, V. Bhopatkar, S. Colafranceschi[68], M. Hohlmann, H. Kalakhety, D. Noonan, T. Roy, F. Yumiceva

University of Illinois at Chicago (UIC), Chicago, USA
M.R. Adams, L. Apanasevich, D. Berry, R.R. Betts, I. Bucinskaite, R. Cavanaugh, O. Evdokimov, L. Gauthier, C.E. Gerber, D.J. Hofman, P. Kurt, C. O'Brien, I.D. Sandoval Gonzalez, P. Turner, N. Varelas, Z. Wu, M. Zakaria, J. Zhang

The University of Iowa, Iowa City, USA
B. Bilki[69], W. Clarida, K. Dilsiz, S. Durgut, R.P. Gandrajula, M. Haytmyradov, V. Khristenko, J.-P. Merlo, H. Mermerkaya[70], A. Mestvirishvili, A. Moeller, J. Nachtman, H. Ogul, Y. Onel, F. Ozok[71], A. Penzo, C. Snyder, E. Tiras, J. Wetzel, K. Yi

Johns Hopkins University, Baltimore, USA
I. Anderson, B. Blumenfeld, A. Cocoros, N. Eminizer, D. Fehling, L. Feng, A.V. Gritsan, P. Maksimovic, M. Osherson, J. Roskes, U. Sarica, M. Swartz, M. Xiao, Y. Xin, C. You

The University of Kansas, Lawrence, USA
P. Baringer, A. Bean, C. Bruner, J. Castle, R.P. Kenny III, A. Kropivnitskaya, D. Majumder, M. Malek, W. Mcbrayer, M. Murray, S. Sanders, R. Stringer, Q. Wang

Kansas State University, Manhattan, USA
A. Ivanov, K. Kaadze, S. Khalil, M. Makouski, Y. Maravin, A. Mohammadi, L.K. Saini, N. Skhirtladze, S. Toda

Lawrence Livermore National Laboratory, Livermore, USA
D. Lange, F. Rebassoo, D. Wright

University of Maryland, College Park, USA
C. Anelli, A. Baden, O. Baron, A. Belloni, B. Calvert, S.C. Eno, C. Ferraioli, J.A. Gomez, N.J. Hadley, S. Jabeen, R.G. Kellogg, T. Kolberg, J. Kunkle, Y. Lu, A.C. Mignerey, Y.H. Shin, A. Skuja, M.B. Tonjes, S.C. Tonwar

Massachusetts Institute of Technology, Cambridge, USA
A. Apyan, R. Barbieri, A. Baty, R. Bi, K. Bierwagen, S. Brandt, W. Busza, I.A. Cali, Z. Demiragli, L. Di Matteo, G. Gomez Ceballos, M. Goncharov, D. Gulhan, D. Hsu, Y. Iiyama, G.M. Innocenti,

M. Klute, D. Kovalskyi, K. Krajczar, Y.S. Lai, Y.-J. Lee, A. Levin, P.D. Luckey, A.C. Marini, C. Mcginn, C. Mironov, S. Narayanan, X. Niu, C. Paus, C. Roland, G. Roland, J. Salfeld-Nebgen, G.S.F. Stephans, K. Sumorok, K. Tatar, M. Varma, D. Velicanu, J. Veverka, J. Wang, T.W. Wang, B. Wyslouch, M. Yang, V. Zhukova

University of Minnesota, Minneapolis, USA
A.C. Benvenuti, B. Dahmes, A. Evans, A. Finkel, A. Gude, P. Hansen, S. Kalafut, S.C. Kao, K. Klapoetke, Y. Kubota, Z. Lesko, J. Mans, S. Nourbakhsh, N. Ruckstuhl, R. Rusack, N. Tambe, J. Turkewitz

University of Mississippi, Oxford, USA
J.G. Acosta, S. Oliveros

University of Nebraska-Lincoln, Lincoln, USA
E. Avdeeva, R. Bartek, K. Bloom, S. Bose, D.R. Claes, A. Dominguez, C. Fangmeier, R. Gonzalez Suarez, R. Kamalieddin, D. Knowlton, I. Kravchenko, F. Meier, J. Monroy, F. Ratnikov, J.E. Siado, G.R. Snow, B. Stieger

State University of New York at Buffalo, Buffalo, USA
M. Alyari, J. Dolen, J. George, A. Godshalk, C. Harrington, I. Iashvili, J. Kaisen, A. Kharchilava, A. Kumar, A. Parker, S. Rappoccio, B. Roozbahani

Northeastern University, Boston, USA
G. Alverson, E. Barberis, D. Baumgartel, M. Chasco, A. Hortiangtham, A. Massironi, D.M. Morse, D. Nash, T. Orimoto, R. Teixeira De Lima, D. Trocino, R.-J. Wang, D. Wood, J. Zhang

Northwestern University, Evanston, USA
S. Bhattacharya, K.A. Hahn, A. Kubik, J.F. Low, N. Mucia, N. Odell, B. Pollack, M.H. Schmitt, K. Sung, M. Trovato, M. Velasco

University of Notre Dame, Notre Dame, USA
N. Dev, M. Hildreth, C. Jessop, D.J. Karmgard, N. Kellams, K. Lannon, N. Marinelli, F. Meng, C. Mueller, Y. Musienko[39], M. Planer, A. Reinsvold, R. Ruchti, N. Rupprecht, G. Smith, S. Taroni, N. Valls, M. Wayne, M. Wolf, A. Woodard

The Ohio State University, Columbus, USA
L. Antonelli, J. Brinson, B. Bylsma, L.S. Durkin, S. Flowers, A. Hart, C. Hill, R. Hughes, W. Ji, B. Liu, W. Luo, D. Puigh, M. Rodenburg, B.L. Winer, H.W. Wulsin

Princeton University, Princeton, USA
O. Driga, P. Elmer, J. Hardenbrook, P. Hebda, S.A. Koay, P. Lujan, D. Marlow, T. Medvedeva, M. Mooney, J. Olsen, C. Palmer, P. Piroué, D. Stickland, C. Tully, A. Zuranski

University of Puerto Rico, Mayaguez, USA
S. Malik

Purdue University, West Lafayette, USA
A. Barker, V.E. Barnes, D. Benedetti, L. Gutay, M.K. Jha, M. Jones, A.W. Jung, K. Jung, D.H. Miller, N. Neumeister, B.C. Radburn-Smith, X. Shi, J. Sun, A. Svyatkovskiy, F. Wang, W. Xie, L. Xu

Purdue University Calumet, Hammond, USA
N. Parashar, J. Stupak

Rice University, Houston, USA
A. Adair, B. Akgun, Z. Chen, K.M. Ecklund, F.J.M. Geurts, M. Guilbaud, W. Li, B. Michlin, M. Northup, B.P. Padley, R. Redjimi, J. Roberts, J. Rorie, Z. Tu, J. Zabel

University of Rochester, Rochester, USA
B. Betchart, A. Bodek, P. de Barbaro, R. Demina, Y.t. Duh, Y. Eshaq, T. Ferbel, M. Galanti, A. Garcia-Bellido, J. Han, O. Hindrichs, A. Khukhunaishvili, K.H. Lo, P. Tan, M. Verzetti

Rutgers, The State University of New Jersey, Piscataway, USA
J.P. Chou, E. Contreras-Campana, Y. Gershtein, T.A. Gómez Espinosa, E. Halkiadakis, M. Heindl, D. Hidas, E. Hughes, S. Kaplan, R. Kunnawalkam Elayavalli, S. Kyriacou, A. Lath, K. Nash, H. Saka, S. Salur, S. Schnetzer, D. Sheffield, S. Somalwar, R. Stone, S. Thomas, P. Thomassen, M. Walker

University of Tennessee, Knoxville, USA
M. Foerster, J. Heideman, G. Riley, K. Rose, S. Spanier, K. Thapa

Texas A&M University, College Station, USA
O. Bouhali[72], A. Castaneda Hernandez[72], A. Celik, M. Dalchenko, M. De Mattia, A. Delgado, S. Dildick, R. Eusebi, J. Gilmore, T. Huang, T. Kamon[73], V. Krutelyov, R. Mueller, I. Osipenkov, Y. Pakhotin, R. Patel, A. Perloff, L. Perniè, D. Rathjens, A. Rose, A. Safonov, A. Tatarinov, K.A. Ulmer

Texas Tech University, Lubbock, USA
N. Akchurin, C. Cowden, J. Damgov, C. Dragoiu, P.R. Dudero, J. Faulkner, S. Kunori, K. Lamichhane, S.W. Lee, T. Libeiro, S. Undleeb, I. Volobouev, Z. Wang

Vanderbilt University, Nashville, USA
E. Appelt, A.G. Delannoy, S. Greene, A. Gurrola, R. Janjam, W. Johns, C. Maguire, Y. Mao, A. Melo, H. Ni, P. Sheldon, S. Tuo, J. Velkovska, Q. Xu

University of Virginia, Charlottesville, USA
M.W. Arenton, P. Barria, B. Cox, B. Francis, J. Goodell, R. Hirosky, A. Ledovskoy, H. Li, C. Neu, T. Sinthuprasith, X. Sun, Y. Wang, E. Wolfe, F. Xia

Wayne State University, Detroit, USA
C. Clarke, R. Harr, P.E. Karchin, C. Kottachchi Kankanamge Don, P. Lamichhane, J. Sturdy

University of Wisconsin - Madison, Madison, WI, USA
D.A. Belknap, D. Carlsmith, S. Dasu, L. Dodd, S. Duric, B. Gomber, M. Grothe, M. Herndon, A. Hervé, P. Klabbers, A. Lanaro, A. Levine, K. Long, R. Loveless, A. Mohapatra, I. Ojalvo, T. Perry, G.A. Pierro, G. Polese, T. Ruggles, T. Sarangi, A. Savin, A. Sharma, N. Smith, W.H. Smith, D. Taylor, P. Verwilligen, N. Woods

†: Deceased
1: Also at Vienna University of Technology, Vienna, Austria
2: Also at State Key Laboratory of Nuclear Physics and Technology, Peking University, Beijing, China
3: Also at Institut Pluridisciplinaire Hubert Curien, Université de Strasbourg, Université de Haute Alsace Mulhouse, CNRS/IN2P3, Strasbourg, France
4: Also at Universidade Estadual de Campinas, Campinas, Brazil
5: Also at Centre National de la Recherche Scientifique (CNRS) - IN2P3, Paris, France
6: Also at Université Libre de Bruxelles, Bruxelles, Belgium
7: Also at Laboratoire Leprince-Ringuet, Ecole Polytechnique, IN2P3-CNRS, Palaiseau, France

8: Also at Joint Institute for Nuclear Research, Dubna, Russia

9: Also at Suez University, Suez, Egypt

10: Now at British University in Egypt, Cairo, Egypt

11: Also at Ain Shams University, Cairo, Egypt

12: Also at Cairo University, Cairo, Egypt

13: Now at Helwan University, Cairo, Egypt

14: Also at Université de Haute Alsace, Mulhouse, France

15: Also at CERN, European Organization for Nuclear Research, Geneva, Switzerland

16: Also at Skobeltsyn Institute of Nuclear Physics, Lomonosov Moscow State University, Moscow, Russia

17: Also at Tbilisi State University, Tbilisi, Georgia

18: Also at RWTH Aachen University, III. Physikalisches Institut A, Aachen, Germany

19: Also at University of Hamburg, Hamburg, Germany

20: Also at Brandenburg University of Technology, Cottbus, Germany

21: Also at Institute of Nuclear Research ATOMKI, Debrecen, Hungary

22: Also at MTA-ELTE Lendület CMS Particle and Nuclear Physics Group, Eötvös Loránd University, Budapest, Hungary

23: Also at University of Debrecen, Debrecen, Hungary

24: Also at Indian Institute of Science Education and Research, Bhopal, India

25: Also at University of Visva-Bharati, Santiniketan, India

26: Now at King Abdulaziz University, Jeddah, Saudi Arabia

27: Also at University of Ruhuna, Matara, Sri Lanka

28: Also at Isfahan University of Technology, Isfahan, Iran

29: Also at University of Tehran, Department of Engineering Science, Tehran, Iran

30: Also at Plasma Physics Research Center, Science and Research Branch, Islamic Azad University, Tehran, Iran

31: Also at Laboratori Nazionali di Legnaro dell'INFN, Legnaro, Italy

32: Also at Università degli Studi di Siena, Siena, Italy

33: Also at Purdue University, West Lafayette, USA

34: Now at Hanyang University, Seoul, Korea

35: Also at International Islamic University of Malaysia, Kuala Lumpur, Malaysia

36: Also at Malaysian Nuclear Agency, MOSTI, Kajang, Malaysia

37: Also at Consejo Nacional de Ciencia y Tecnología, Mexico city, Mexico

38: Also at Warsaw University of Technology, Institute of Electronic Systems, Warsaw, Poland

39: Also at Institute for Nuclear Research, Moscow, Russia

40: Now at National Research Nuclear University 'Moscow Engineering Physics Institute' (MEPhI), Moscow, Russia

41: Also at St. Petersburg State Polytechnical University, St. Petersburg, Russia

42: Also at University of Florida, Gainesville, USA

43: Also at Faculty of Physics, University of Belgrade, Belgrade, Serbia

44: Also at INFN Sezione di Roma; Università di Roma, Roma, Italy

45: Also at National Technical University of Athens, Athens, Greece

46: Also at Scuola Normale e Sezione dell'INFN, Pisa, Italy

47: Also at National and Kapodistrian University of Athens, Athens, Greece

48: Also at Riga Technical University, Riga, Latvia

49: Also at Institute for Theoretical and Experimental Physics, Moscow, Russia

50: Also at Albert Einstein Center for Fundamental Physics, Bern, Switzerland

51: Also at Adiyaman University, Adiyaman, Turkey

52: Also at Mersin University, Mersin, Turkey

53: Also at Cag University, Mersin, Turkey
54: Also at Piri Reis University, Istanbul, Turkey
55: Also at Gaziosmanpasa University, Tokat, Turkey
56: Also at Ozyegin University, Istanbul, Turkey
57: Also at Izmir Institute of Technology, Izmir, Turkey
58: Also at Marmara University, Istanbul, Turkey
59: Also at Kafkas University, Kars, Turkey
60: Also at Istanbul Bilgi University, Istanbul, Turkey
61: Also at Yildiz Technical University, Istanbul, Turkey
62: Also at Hacettepe University, Ankara, Turkey
63: Also at Rutherford Appleton Laboratory, Didcot, United Kingdom
64: Also at School of Physics and Astronomy, University of Southampton, Southampton, United Kingdom
65: Also at Instituto de Astrofísica de Canarias, La Laguna, Spain
66: Also at Utah Valley University, Orem, USA
67: Also at University of Belgrade, Faculty of Physics and Vinca Institute of Nuclear Sciences, Belgrade, Serbia
68: Also at Facoltà Ingegneria, Università di Roma, Roma, Italy
69: Also at Argonne National Laboratory, Argonne, USA
70: Also at Erzincan University, Erzincan, Turkey
71: Also at Mimar Sinan University, Istanbul, Istanbul, Turkey
72: Also at Texas A&M University at Qatar, Doha, Qatar
73: Also at Kyungpook National University, Daegu, Korea